Phosphatidylcholine biosynthesis in Mitis group streptococci via a host metabolite scavenging pathway

Luke R. Joyce[1], Ziqiang Guan[2]*, and Kelli L. Palmer[1]*

Department of Biological Sciences, The University of Texas at Dallas, Richardson, Texas, USA[1], Department of Biochemistry, Duke University Medical Center, Durham, NC[2]

*Corresponding authors:

Ziqiang Guan: Ziqiang.Guan@duke.edu

Kelli Palmer: Kelli.Palmer@utdallas.edu

Abstract

The Mitis group streptococci include the major human pathogen *Streptococcus pneumoniae* and the oral opportunistic pathogens *S. mitis* and *S. oralis* which are primary colonizers in the oral cavity and agents of bacteremia and infective endocarditis in immunocompromised patients. Bacterial membrane lipids play crucial roles in microbe-host interactions, yet for many pathogens, the composition of the membrane is poorly understood. In this study, we characterized the lipidomes of selected species of Mitis group streptococci and investigated the mechanistic basis for biosynthesis of the phospholipid phosphatidylcholine (PC). PC is a major lipid in eukaryotic cellular membranes, but it is considered to be comparatively rare in bacterial taxa. Using liquid chromatography/mass spectrometry (LC/MS) in conjunction with stable isotope tracing, we determined that Mitis group streptococci synthesize PC via the rare host metabolite scavenging pathway, the glycerophosphocholine (GPC) pathway, which is largely uncharacterized in bacteria. Furthermore, we identify the acyltransferase, PlsC, as playing a major role in the pathway by acylating lysoPC to PC. Our work demonstrates that Mitis group streptococci including *S. pneumoniae* remodel their membrane in response to the major human metabolites GPC and lysoPC.

Key words

Phosphatidylcholine, phospholipid, *Streptococcus pneumoniae, Streptococcus mitis, Streptococcus oralis*, Mitis group streptococci, glycerophosphocholine

Significance

We lack fundamental information about the structure of the cellular membrane even for the best studied pathogens of critical significance for human health. The Mitis group streptococci are closely linked to humans in health and disease. Here, we demonstrate that these streptococci scavenge major human metabolites and use them to synthesize the membrane phospholipid phosphatidylcholine. Our work is significant because it identifies a mechanism by which the major human pathogen *S. pneumoniae* and the primary human oral colonizers *S. mitis* and *S. oralis* remodel their membrane in response to the host.

Introduction

The Mitis group streptococci are Gram-positive bacteria that natively inhabit the human oral cavity, nasopharynx, and gastrointestinal tract (1). They include the species *S. mitis* and *S. oralis*, which are among the first colonizers of the human oral cavity from birth and are believed to play important roles in host-microbe-microbe interactions by creating an anchor for biofilm formation with other oral microbiota (2, 3). They are also opportunistic pathogens causing bacteremia and infective endocarditis (4–7). They also include the major human pathogen, *S. pneumoniae*. *S. pneumoniae* has >99% 16S rRNA sequence identity with *S. mitis* and *S. oralis* (8–10), and with which they exchange capsule biosynthesis and antibiotic resistance genes (11, 12) and show antibody cross-reactivity (13).

We, and others, recently reported that Mitis group streptococci have unusual membrane physiology in that they can proliferate while lacking the major anionic phospholipids phosphatidylglycerol (PG) and cardiolipin (CL) (14, 15). More specifically, *S. mitis* and *S. oralis* can tolerate deletion or inactivation of *cdsA*, the gene encoding phosphatidate cytidylyltransferase (14, 15). CdsA catalyzes synthesis of cytidine diphosphate-diacylglycerol (CDP-DAG), a key intermediate in the synthesis of major phospholipids (Figure 1). Deletion or inactivation of *cdsA* in Mitis group streptococci, and the corresponding loss of PG and CL, confers high-level (MIC >256 µg/mL) resistance to daptomycin (DAP), a last-line lipopetide antibiotic (14–16).

Unexpectedly, lipidomic analysis of Mitis group streptococci by normal phase liquid chromatography – electrospray ionization/mass spectrometry (NPLC-ESI/MS) revealed the presence of phosphatidylcholine (PC) in the wild-type and in *cdsA* null mutants (14). To our knowledge, PC in streptococci had not been previously described. Overall, the lipid compositions of streptococci are under-studied and poorly characterized. Previous studies analyzing lipids of streptococci primarily used thin layer chromatography, whose limitations in analytical sensitivity and molecular specificity prohibit comprehensive lipidomic identification; these studies did not detect PC (17–22). However, PC is a biologically significant lipid. As a zwitterionic phospholipid, PC promotes bilayer formation (23), reduces the rate of protein folding to allow for correct protein configurations (24, 25), aids in resistance to antimicrobials targeting prokaryotic membranes (26), aids in surviving environmental fluctuations such as temperature shifts (27), and is a major component of eukaryotic membranes. There is evidence that PC plays important roles in host-microbe interactions. *Legionella* lacking functional PC biosynthesis exhibit decreased virulence because of poor recognition by host macrophages and reduced motility (28). *Brucella abortus* and *Agrobacterium tumefaciens* also exhibit diminished virulence when PC biosynthesis is inactivated (29–31). Alternatively, *Pseudomonas aeruginosa* strains lacking PC show no detectable alteration in virulence (32).

Because PC may impact how Mitis group streptococci interact with the human host, we sought to investigate the mechanism for PC biosynthesis in these organisms. There are four experimentally confirmed PC biosynthesis pathways in bacteria (Figure 1), two of

which are widespread and well-characterized, namely the phosphatidylethanolamine (PE) methylation pathway (23, 33), and the phosphatidylcholine synthase (Pcs) pathway (34, 35). The PE methylation pathway uses PE as a starting substrate, which is methylated via phospholipid *N*-methyltransferase (Pmt) in three subsequent steps to form monomethylPE (MMPE), dimethylPE (DMPE), and finally PC, using *S*-adenosylmethionine as the methyl group donor (33). The PE methylation pathway is utilized by mammalian liver cells (23, 36) and bacteria including *Rhodobacter sphaeroides* and *Sinorhizobium meliloti* (23). The Pcs pathway is exclusive to prokaryotes and is a one-step reaction in which a phosphatidylcholine synthase (Pcs) enzyme condenses choline with CDP-DAG to form PC (34). The presence of either *pmt* or *pcs* genes has been used to identify bacterial taxa likely to produce PC (23).

A third pathway, the CDP-choline pathway (referred to as the Kennedy pathway in eukaryotes), was recently identified in the Gram-negative human oral colonizer, *Treponema denticola* (37). In this pathway, choline is scavenged from the environment and activated to CDP-choline via the LicAC enzymes. Many host-associated bacteria possess LicAC and utilize host-derived choline to decorate a wide range of extracellular structures (23) including the Type IV lipoteichoic acid of *S. pneumoniae, S. mitis*, and *S. oralis* (38–42). In the CDP-choline pathway, CDP-choline is condensed with diacylglycerol (DAG) by a 1,2-diacylglycerol choline phosphotransferase (CPT) to form PC.

A fourth pathway, the glycerophosphocholine (GPC) pathway, has been reported for only two organisms: the Gram-negative plant pathogen *Xanthomonas campestris* (43) and yeast (44). In eukaryotic cells, GPC is a breakdown product of choline-containing membrane phospholipids. Yeast can utilize GPC as the source for glycerol-3-phosphate, choline, or phosphate depending on the environmental conditions (45). GPC is a major human metabolite present in saliva and blood (46, 47). In the GPC pathway, GPC is scavenged from the environment and acylated twice to form the intermediate lysoPC (LPC) and then PC. The genetics underlying the GPC pathway in *X. campestris* have not been fully elucidated. Moser *et al*. identified two *X. campestris* acyltransferases that performed the second acylation event from LPC to PC (43). Yeast possess a fully elucidated GPC pathway (44, 48).

Here we use NPLC-ESI/MS and other biochemical and genetic approaches to investigate PC biosynthesis in Mitis group streptococci using type strains and an infective endocarditis isolate (Table 1). We determined that these organisms synthesize PC by the rare GPC pathway via scavenging the host metabolites GPC and LPC.

Results

PC biosynthesis by Mitis group streptococci. We previously reported lipidomic analysis by NPLC-ESI/MS of three Mitis group infective endocarditis isolates cultured in the rich, undefined laboratory growth medium Todd Hewitt broth (THB). We determined that these organisms possess PC in their membranes ((14) and Table 1). We

confirmed these results using the *S. mitis* and *S. oralis* type strains ATCC 49456 and ATCC 35037, respectively (Table 1).

In this study, we used one of the infective endocarditis isolates, referred to as SM43, for most of our mechanistic studies of PC biosynthesis. Phylogenetic assignments within the Mitis group are difficult due to variable phenotypes and highly conserved 16S rRNA sequences (8, 9). SM43 was initially assigned to the *S. mitis* species using standard biochemical techniques (49). In this study, we analyzed a complete SM43 genome sequence using an average nucleotide identity (ANI) calculator (50, 51). ANI values are used for molecular species definitions (52), and two bacterial strains with an ANI of ≥95% in their shared genes are considered to be the same species and with an ANI of >70% are considered to be the same genus (53, 54). We compared the SM43 genome with those of *S. oralis* ATCC 35037 and *S. mitis* ATCC 49456. SM43 possesses 94.32% ANI with *S. oralis* ATCC 35037 and 86.86% ANI with *S. mitis* ATCC 49456. Based on these data showing a close phylogenetic relationship between SM43 and *S. oralis*, we refer to SM43 as a Mitis group *Streptococcus* in this study (Table 1).

PC biosynthesis in SM43 is not by the PE methylation pathway or Pcs pathway.

The well-characterized PE methylation pathway for PC biosynthesis is catalyzed by the enzyme Pmt (Figure 1). This pathway is excluded as SM43 does not synthesize PE (14), nor does it encode *pmt*.

The Pcs pathway requires CDP-DAG and choline as substrates (Figure 1). CdsA catalyzes the synthesis of CDP-DAG (Figure 1). As we and others have published previously, *cdsA* loss-of-function mutants in Mitis group streptococci do not synthesize CDP-DAG, resulting in the loss of the major anionic phospholipids PG and CL and the accumulation of PA in the membrane (14, 15). In our previous study, we detected PC in strains with *cdsA* point mutations arising spontaneously under DAP selection. To confirm these results, we generated a clean deletion of *cdsA* in SM43. PC was detected in both wild-type and Δ*cdsA* SM43 cultured in THB. Figure 2a shows the relative abundance of PC in the SM43 membrane during mid-exponential phase. The ESI/MS spectra of the major PC species, PC (30:1) at *m/z* 704, PC (32:1) at *m/z* 732, PC (34:1) at *m/z* 760, and PC(36:2) at *m/z* 786 are shown for SM43 (Figure 2b) and *S. mitis* type strain ATCC 49456 (Supp. Fig. 1a). The chemical structure of PC (34:1) shown in (Figure 2c) is supported by MS/MS (Supp. Fig. 1b). The ESI/MS spectra of PC in SM43Δ*cdsA* is shown in (Figure 2d), Based on these results and the absence of a *pcs* ortholog in the SM43 and ATCC 49456 genomes (Figure 1) the *pcs* pathway is excluded.

SM43 encodes a partial CDP-choline pathway. The CDP-choline pathway (referred to as the Kennedy pathway in eukaryotic organisms) requires the activation of choline to CDP-choline by the LicA and LicC enzymes. This is followed by condensation of CDP-choline with DAG by a 1,2-diacylglycerol choline phosphotransferase (CPT) enzyme to form PC (Figure 1). *S. mitis* and *S. oralis* encode *licABC* for the activation of exogenous choline to CDP-choline, which is required for choline decoration of Type IV lipoteichoic

acid (LTA) in these organisms and *S. pneumoniae* (38–42). Given that SM43 encodes *licABC*, we assessed the possibility that the CDP-choline pathway is used for PC biosynthesis in this organism.

The CPT of *T. denticola* possesses a CDP-alcohol phosphatidyltransferase domain (Superfamily accession: cl00453) (37). Only one SM43 predicted protein, phosphatidylglycerophosphate synthase (PgsA), possesses this domain. PgsA catalyzes the addition of glycerolphosphate to CDP-DAG to form phosphatidylglycerophosphate (PG-P) (55) which is required for subsequent PG and CL synthesis (Figure 1).

To investigate if PgsA has the CPT activity (or substrate promiscuity) in SM43, a 284 bp region of *pgsA* encoding the catalytic domain was replaced with an erythromycin resistance cassette. The replacement of *pgsA* was confirmed by whole genome sequencing. The *pgsA* mutant has a significant growth defect, with a doubling time almost twice that of the wild type (Supp. Fig. 2). The defect is likely due to PgsA interaction with RodZ in membrane homeostasis, as has been reported for *Bacillus subtilis* (56). Similar to SM43Δ*cdsA*, PC is present in SM43Δ*pgsA* cultured in THB (Figure 2e). As expected, the SM43Δ*pgsA* mutant lacks PG and CL (Table 1) and is high-level DAP resistant (MIC of >256 µg/mL) (Table S1), in agreement with similar experiments by Tran et al 2019. utilizing *S. mitis-oralis* strains (57). We conclude that the sole candidate for CPT activity in SM43, PgsA, does not catalyze PC biosynthesis.

To conclusively exclude the CDP-choline pathway, we performed stable isotope-labeling experiments. SM43 was cultured in THB supplemented with 2 mM deuterated choline (choline-*d9*), in which all nine hydrogen (1 Da) atoms on the three methyl groups are replaced with deuterium (2 Da) atoms, increasing the mass of choline by 9 Da. If SM43 utilizes the CDP-choline pathway for PC biosynthesis, an *m/z* shift of 9 Da would be observed for CDP-choline and PC species in SM43 grown in choline-*d9*-supplemented cultures. As expected, we observed choline-*d9* incorporation into CDP-choline via a shift of its M^+ ion from *m/z* 489 (Figure 3a; no choline-*d9* supplementation) to *m/z* 498 (Figure 3b, with choline-*d9* supplementation). The identification of CDP-choline and CDP-choline-*d9* was confirmed by MS/MS (Supp. Fig. 3). In contrast, no *m/z* shift was observed for PC species between control (Figure 3c) and choline-*d9*-supplemented (Figure 3d) cultures. These data definitively eliminate the CDP-choline pathway as the SM43 PC biosynthesis pathway.

SM43 utilizes the GPC scavenge pathway for PC biosynthesis. GPC is a major human metabolite, present in blood and saliva at concentrations up to 40 µM and 10 µM respectively (46). Using reverse-phase LC/MS, we detected GPC (*m/z* 258.1) in THB (Supp. Fig. 4), likely from the heart infusion component of the medium.

To determine whether SM43 utilizes the GPC pathway for PC biosynthesis, we used stable isotope-labeled GPC to trace the conversion of GPC into PC. Specifically, SM43 was cultured in THB with and without 0.13 mM GPC-*d9* supplementation. A *m/z* shift of 9 Da was observed for all PC species (Figure 4a), demonstrating that SM43 uses the

GPC pathway for PC biosynthesis. To further confirm this result, SM43 and *S. mitis* ATCC 49456 were cultured in a chemically defined medium containing 0.5 mM choline (DM) (58, 59), with and without 0.13 mM GPC supplementation. SM43 and ATCC 49456 synthesize PC only when GPC is present in the defined medium (Figure 5 and Table 2). Taken together, GPC-*d9* isotope tracking and defined medium experiments independently confirm that SM43 utilizes the GPC pathway for PC biosynthesis. Moreover, these results are not strain-specific, as the *S. mitis* type strain also synthesizes PC only when GPC is present in the growth environment.

PC is not an essential component in the lipid membrane for SM43 and ATCC 49456, evidenced by their abilities to grow in DM lacking GPC. To assess the impact that PC has on growth dynamics, SM43 and ATCC 49456 were cultured in THB and in DM with and without GPC supplementation. There is no impact on growth of either strain when GPC was present or absent from the media (Supp. Fig. 5).

Since LPC is an intermediate in the GPC pathway, we hypothesized that SM43 could also scavenge LPC from its environment. LPC is present in human blood at up to 200 µM (60). We supplemented THB with LPC (20:0), which has an acyl chain that is not usually observed in bacterial membranes. SM43 readily scavenged exogenous LPC (20:0) and acylated it to form PC (Figure 4b). We conclude that SM43 scavenges both GPC and LPC from its environment to synthesize PC.

SM43 acyltransferase PlsC acylates LPC to form PC. A functional GPC pathway requires transporters to transport GPC or LPC into the cell, and at least one acyltransferase to add acyl chains, in an acyl-CoA dependent manner, to ultimately form PC (Figure 6). As a starting point, we focused our efforts on identifying an acyltransferase catalyzing acylation of LPC to form PC. SM43 encodes two predicted acyltransferases, PlsY and PlsC (Figure 1). In *S. pneumoniae*, PlsY has been determined as essential by Tn-seq (61) and PlsC determined to be essential by gene disruption (62). Because PlsY and PlsC are likely to also be essential in SM43, we utilized a heterologous expression approach to test whether these enzymes participate in PC biosynthesis.

An expression system in *Enterococcus faecalis* T11 was designed to assess SM43 acyltransferase activities. We selected this strain because *E. faecalis* does not synthesize PC (63, 64). SM43 *plsY* and *plsC* were expressed constitutively from an *E. faecalis bacA* promoter on the multicopy vector pGR-*ermB* (65). Recombinant *E. faecalis* strains were cultured in brain heart infusion (BHI) broth supplemented with 2 mg LPC (15:0) and chloramphenicol, and lipidomics analysis performed. However, we observed high phospholipase activity in the *E. faecalis* T11 cells that rapidly degrades LPC (15:0).

To overcome the high phospholipase activity of live *E. faecalis* T11 cells, a crude extract assay was performed on overnight cultures of *E. faecalis* T11(pGR-EV) (empty vector), T11(pGR-PlsY), and T11(pGR-PlsC). For the *in vitro* assay, 400 µL of the crude extract

was added to 400 µL reaction mixture containing 0.08 mg LPC 20:0 and 0.16 mg palmitoyl-CoA, and incubated for 60 min at 30°C before acidic Bligh-Dyer extraction and analysis by NPLC-ESI/MS. Extracted ion chromatograms (XIC's) for PC (20:0/16:0) *m/z* 790 are shown in Figure 7. Basal levels of PC (20:0/16:0) are observed in T11(pGR-EV) (Figure 7a), and T11(pGR-PlsY) (Figure 7c) at approximately 0.5×10^3 counts per second (cps). However, in T11(pGR-PlsC), the PC (20:0/16:0) is orders of magnitude higher, at 1.15×10^5 cps (Figure 7b). ESI/MS of PC (20:0/16:0) at *m/z* 790 for T11(pGR-EV), T11(pGR-PlsY), and T11(pGR-PlsC) is shown in Supp. Fig. 6. To indicate the relative abundance of membrane present during *in vitro* reactions, XIC for the co-eluting lipid lysyl-PG are shown in Supp. Fig. 7. Similar levels of lysyl-PG present during *in vitro* reactions indicate that the LPC-to-PC acylation activity of PlsC is not due to an increased cell density. Overall, these data indicate that SM43 PlsC plays a significant role in PC formation in SM43 by catalyzing the acylation of LPC, forming PC. We next sought to confirm this *in vitro* result by constructing a SM43 *plsC* deletion mutant. However, multiple attempts to delete *plsC* from SM43 were unsuccessful, likely because this acyltransferase is required for the synthesis of PA which is known to be essential in all organisms (Figure 1).

GPC-dependent PC synthesis by *S. pneumoniae and S. oralis*. *S. pneumoniae* is a major human pathogen and a close relative of *S. mitis*. Surprisingly, there are only a few reports on lipid analysis of *S. pneumoniae* (17–19), for which thin layer chromatography was used as the analytical technique. We applied LC-ESI/MS, with much higher sensitivity and specificity, to investigate the lipidome of *S. pneumoniae*. Remarkably, PC

is present in the membranes of *S. pneumoniae* D39 (Figure 8a,b) and TIGR4 (Figure 8c,d) cultured in THB supplemented with yeast extract (also see Table 1). Figure 8a and c shows the positive ion TIC and the relative abundance of PC in the D39 and TIGR4, respectively, in early stationary phase. The ESI/MS spectra of the major PC species, PC (30:1) at *m/z* 704, PC (32:1) at *m/z* 732, PC (34:2) at *m/z* 758, and PC(36:2) at *m/z* 786 are shown for D39 (Figure 8b) and TIGR4 (Figure 8d). Previously, we identified PC present in infective endocarditis *S. oralis* isolates 1647 and 1648 (14). To determine if *S. pneumoniae* and *S. oralis* utilize the GPC pathway for PC biosynthesis, *S. pneumoniae* D39 and *S. oralis* ATCC 35037 were cultured in defined media with and without GPC supplementation. When GPC is not available, *S. pneumoniae* and *S. oralis* do not synthesize PC (Figure 9a,c). PC is only present when GPC is available in the exogenous environment (Figure 9b,d). We conclude that *S. pneumoniae* and *S. oralis* also scavenge GPC from the media to synthesize PC.

Discussion

The lipid membrane is a dynamic site of interaction between microbial pathogens and their hosts. However, for many pathogens, the composition of the membrane is poorly understood. In this study, we characterized the lipidomes of selected species of Mitis group streptococci and investigated the mechanistic basis for biosynthesis of the phospholipid PC. We found that Mitis group streptococci remodel their membrane lipid compositions in response to the host metabolites GPC and LPC. To our knowledge, this is the first description of PC in *S. pneumoniae,* a major human pathogen which has been studied for over a century and yet its membrane lipid composition remains poorly

understood. There have been very few lipidomic studies performed in *S. pneumoniae* (17–19), and little is known about how *S. pneumoniae* remodels its membrane in response to changing environments inside and outside the host. Here, we reported the first identification of PC in *S. pneumoniae* and demonstrated that *S. pneumoniae* synthesizes PC only when GPC, a major human metabolite, is available for scavenge.

Very little is known about the GPC pathway in bacteria. In this study we investigated whether we could identify an acyltransferase involved in this pathway, since that approach was successful for the only other bacterium reported to possess this pathway to date. Specifically, two acyltransferases in *X. campestris* were experimentally confirmed to acylate LPC to PC (43). Through the use of *in vitro* cell lysate reactions, we show that the SM43 acyltransferase, PlsC, has LPC acylation activity. The well-characterized activity of PlsC is its addition of a second acyl chain onto LPA to form PA, which is the initial substrate in anionic phospholipid biosynthesis (66). We did not experimentally confirm whether SM43 PlsC catalyzes acylation of both LPA and LPC; however, we hypothesize this to be the case. The only crystal structure available for PlsC is from the hyperthermophiliic bacterium *Thermotoga maritima* (67), with which the SM43 PlsC shares only weak (24%) amino acid sequence similarity. Biochemical studies of purified SM43 PlsC and structural modeling of this enzyme in comparison with PlsC from other bacteria will be required to understand the mechanistic basis for SM43 PlsC acylation of LPC.

A complete GPC pathway has been characterized in yeast (44, 48). It includes a dual substrate transporter, Git1, for the uptake of glycerophosphoinositol and GPC; a previously unidentified GPC acyltransferase referred to as Gpc1; and the acyltransferase Ale1 performing LPC acylation. To fully elucidate the GPC pathway in streptococci, identification of transporters for GPC and LPC as well as the GPC acyltransferase are required. However, no orthologs of the yeast GPC pathway components were identified in the SM43 genome. Given the roles of PlsX and PlsY in acylation of glycerol-3-phosphate, these enzymes may also acylate GPC in SM43. In *Mycobacterium tuberculosis,* a sugar-binding ABC transporter, UgpABCE, transports GPC (68). The UgpB substrate binding domain is flexible in substrate affinity, binding to phosphate-containing substrates such as *sn*-glycerol 3-phopshate, glycerol 2-phosphate, and GPC (68–70). Given the reduced size of streptococcal genomes, it is possible that GPC uptake is also conferred by a transport system with flexible substrate specificity.

Our study raised important questions for future work. First, the relationship between PC levels in the membrane and the availability of GPC and LPC at different human body sites needs to be quantitatively assessed. GPC and LPC levels vary at different sites of the human body and in health and disease (≤ 500 µM and ≤ 200 µM, respectively (46, 60)), and this is particularly relevant to *S. pneumoniae* which can cause aggressive disease at multiple sites including the lung, bloodstream, and meninges. Second, we did not assess whether and how PC levels impact clinically relevant phenotypes such as virulence and antibiotic susceptibility. This is due in part to our limited understanding of

the GPC pathway, which requires elucidation. However, by culturing cells in defined medium with and without GPC, in future studies we can assess the biophysical impact of PC on streptococcal membranes in terms of lipid/microdomain organization, charge, rigidity, and protein composition.

Overall, our work highlights the importance of utilizing laboratory culture media that mimic the *in vivo* nutritional environments where pathogens are found. Our identification of PC in the membrane of Mitis group streptococci including the major human pathogen *S. pneumoniae*, and their utilization of the rare GPC pathway, warrants further investigation into streptococcal membrane biology, about which little is known.

Materials and methods

Bacterial strains, media, and growth conditions. Strains and plasmids used in this study are shown in Table S2. Streptococcal strains were grown in THB in 5% CO_2 at 37°C unless otherwise stated. *S. pneumoniae* THB cultures were supplemented with 0.5% yeast extract. *E. faecalis* were grown in BHI at 37°C. *Escherichia coli* was routinely cultured at 37°C in lysogeny broth with agitation at 220 rpm. Streptococcal chemically defined media (58) was diluted from stock as described (59) supplemented with 0.5 mM choline (referred to as DM), slightly modified from (71) unless otherwise stated. Media were supplemented with 130 µM glycerophosphocholine (Sigma-Aldrich) where stated. Antibiotic concentrations used for SM43 were erythromycin, 20 µg/mL, and for *E. faecalis* and *E. coli*, chloramphenicol, 15 µg/mL. Daptomycin susceptibilities

were assessed using daptomycin Etest strips (bioMérieux) on Mueller Hinton Agar plates, per CLSI standards (72).

Genome sequencing and assembly. Genomic DNA was isolated using the Qiagen DNeasy Blood and Tissue kit per the manufacturer's protocol with the exception that cells were pre-treated with 180 µL 50 mg/mL lysozyme, 25 µL 2500 U/mL mutanolysin, and 15 µL 20 mg/mL pre-boiled RNase A and incubated at 37°C for 2 h. Pacific Biosciences single molecule real time (SMRT) sequencing was performed by the Johns Hopkins Genome Core. The SM43 whole genome was assembled using the Unicyler assembly pipeline (73) combining SMRT long reads generated in this study and Illumina reads we previously generated for SM43 (accession PRJNA354070; (14)). Sequencing of SM43Δ*pgsA* was performed by Molecular Research DNA (Shallowater, Texas) using Illumina Hi-Seq 2x150 paired end reads.

Deletion of SM43 *cdsA*. Primers used in this study are shown in Table S3. The *cdsA* deletion construct was designed essentially as previously described (74, 75). Briefly, approximately 2 Kb flanking regions on either side of the gene were amplified using Phusion polymerase (Thermo Fisher). PCR products were digested with restriction enzymes (New England Biolabs) and ligated using T4 DNA ligase (New England Biolabs). Ligations were amplified by PCR utilizing the 5’ and 3’ most primers with Phusion polymerase to obtain a linear product. The PCR product was analyzed on a 1% agarose gel and extracted using the QIAquick Gel Extraction Kit per the manufacturer's protocol. The linear construct was transformed into SM43 via natural transformation,

412 described below. Transformation plates were incubated overnight. Putative transformant
413 colonies were inoculated into THB and screened via PCR for the clean deletion of *cdsA*.
414 The *cdsA* regions of putative mutants were sequenced for confirmation (Massachusetts
415 General Hospital DNA Core).
416
417 **Deletion and replacement of SM43 *pgsA*.** The strategy was designed and executed
418 as for *cdsA* deletion, except an erythromycin resistance marker with its native promoter
419 was amplified from $pG^{+}host4$ (76) and inserted between the homologous flanking arms
420 to allow for selection-based screening of putative *pgsA* mutants. The resulting construct
421 deleted 284 bp of *pgsA* encoding the catalytically active site, and replaced them with the
422 erythromycin resistance marker.
423
424 **Natural transformation**. The natural transformation protocol was as previously
425 described (75) with minor modifications. Briefly, 100 µL exponential phase pre-cultures
426 (OD_{600} ~0.5) in THB were frozen with an equal volume of 10% glycerol. Precultures
427 were thawed at room temperature and diluted in 900 µL THB. This was further diluted
428 1:50 in pre-warmed 5 mL THB and incubated at 37°C for 45 minutes. 500 µL culture
429 was aliquoted along with 1 µL of 1 mg/mL competence stimulating peptide
430 (DWRISETIRNLIFPRRK) and 1 µg/mL linear DNA construct. Transformation reactions
431 were cultured for 2 h at 37°C in microcentrifuge tubes before plating on THB agar with
432 selection as appropriate.
433

Lipidomics. Unless otherwise noted, lipidomics analyses were performed on overnight cultures in stationary phase. Centrifugation was performed using a Sorvall RC6+ centrifuge. Cultures were pelleted at 4,280 x *g* for 5 min at room temperature. The supernatants were removed and stored at -80°C until acidic Bligh-Dyer lipid extractions were performed as described (77) with minor modifications. Briefly, cell pellets were resuspended in 1X PBS (Sigma-Aldrich) and transferred to Coring Pyrex glass tubes with PTFR-lined caps (VWR), followed by 1:2 vol:vol chloroform:methanol addition. Single phase extractions were vortexed periodically and incubated at room temperature for 15 minutes before 500 x *g* centrifugation for 10 min. A two-phase Bligh-Dyer was achieved by addition of 100 µl 37% HCL, 1 mL $CHCl_3$, and 900 µl of 1X PBS, which was then vortexed and centrifuged for 5 min at 500 x *g.* The lower phase was removed to a new tube and dried under nitrogen before being stored at -80°C prior to lipidomic analysis.

Normal-phase LC was performed on an Agilent 1200 quaternary LC system equipped with an Ascentis silica high-performance liquid chromatography (HPLC) column (5m; 25 cm by 2.1 mm; Sigma-Aldrich) as described previously (77, 78). Briefly, mobile phase A consisted of chloroform-methanol-aqueous ammonium hydroxide (800:195:5, vol/vol), mobile phase B consisted of chloroform-methanol-water-aqueous ammonium hydroxide (600: 340:50:5, vol/vol), and mobile phase C consisted of chloroform-methanol-water-aqueous ammonium hydroxide (450:450:95:5, vol/vol/vol/vol). The elution program consisted of the following: 100% mobile phase A was held isocratically for 2 min, then linearly increased to 100% mobile phase B over 14 min, and held at 100% mobile phase

B for 11 min. The LC gradient was then changed to 100% mobile phase C over 3 min, held at 100% mobile phase C for 3 min, and, finally, returned to 100% mobile phase A over 0.5 min and held at 100% mobile phase A for 5 min. The LC eluent (with a total flow rate of 300 ml/min) was introduced into the ESI source of a high-resolution TripleTOF5600 mass spectrometer (Sciex, Framingham, MA). Instrumental settings for negative-ion ESI and MS/MS analysis of lipid species were as follows: IS = -4,500 V, CUR = 20 psi, GSI = 20 psi, DP = -55 V, and FP = -150V. The MS/MS analysis used nitrogen as the collision gas. Data analysis was performed using Analyst TF1.5 software (Sciex).

Metabolite extractions. Cultures were pelleted at 4,280 x *g* in a Sorvall RC 6+ floor centrifuge at room temperature, washed once with 1X PBS, and transferred to 1.5 mL microcentrifuge tubes. Cells were pelleted and frozen at -80°C until use. Metabolite extraction was performed as previously described (79) with minor modifications. Briefly, cell pellets were resuspended in 300 µL super-chilled methanol:water (vol:vol 4:1) via vortexing and pipetting, and stored on dry ice for 15 min. Suspensions were centrifuged at 17,136 x *g* at 4°C for 5 min in a table top centrifuge. The supernatant was removed to a pre-chilled Corning Pyrex glass tube and kept on dry ice. A further 2 resuspensions in 200 µL methanol:water (vol:vol 4:1) were performed. Pooled supernatants were dried under nitrogen at room temperature and stored at -80°C prior to analysis.

Reverse phase LC-ESI/MS analysis. RPLC-ESI/MS analysis of water-soluble metabolites was performed using a Shimadzu LC system (comprising a solvent

degasser, two LC-10A pumps and a SCL-10A system controller) coupled to a TripleTOF5600 mass spectrometer (Sciex, Framingham, MA). LC was operated at a flow rate of 200 µl/min with a linear gradient as follows: 100% of mobile phase A was held isocratically for 2 min and then linearly increased to 100% mobile phase B over 14 min and held at 100% B for 4 min. Mobile phase A consisted of methanol/acetonitrile/aqueous 1mM ammonium acetate (60/20/20, v/v/v). Mobile phase B consisted of 100% ethanol containing 1 mM ammonium acetate. A Zorbax SB-C8 reversed-phase column (5 µm, 2.1 x 50 mm) was obtained from Agilent (Palo Alto, CA). The LC eluent was introduced into the ESI source of the mass spectrometer. Instrument settings for negative ion ESI/MS and MS/MS analysis of lipid species were as follows: Ion spray voltage (IS) = -4500 V; Curtain gas (CUR) = 20 psi; Ion source gas 1 (GS1) = 20 psi; De-clustering potential (DP) = -55 V; Focusing potential (FP) = -150 V. Data acquisition and analysis were performed using the Analyst TF1.5 software (Sciex, Framingham, MA).

Deuterated isotope (*d9*) and LPC tracking. Deuterated (*d9*) isotope tracking was performed by addition of 2 mM choline-*d9* (Sigma-Aldrich) in 50 mL THB. 3.7 mM glycerophosphocholine-*d9* (Toronto Research Chemicals) was added to 15 mL THB, to yield a final concentration of 130 µM. Cultures were grown in 5% CO_2 at 37°C for 18 h before 10 mL of choline-*d9* culture or 5 mL of glycerophosphocholine-*d9* culture was removed for metabolite extraction and the remaining culture was pelleted for lipid extraction. LPC (20:0) was obtained from Avanti Polar Lipids. Cultures were

supplemented with 2 mg LPC per 15 mL THB, unless otherwise stated, and incubated overnight in 5% CO_2 at 37°C. Lipid extractions were performed as described.

Acyltransferase expression in *E. faecalis*. SM43 acyltransferases were constitutively expressed by the full *bacA* promoter on a modified pGR-*ermB* plasmid (65). To generate the expression constructs, a 3 fragment Gibson assembly, per manufacturer protocols (New England Biolabs), was performed with the RecA_BacA fragment, Cat fragment, and the acyltransferase for each plasmid (see Supp. Fig. 8). 5 µL of the Gibson assembly reaction was chemically transformed into *E. coli* DH5α by heat shock at 42°C for 70 sec before outgrowth in SOC medium for 30 min. Colonies were screened for gene insert using PCR with *Taq* polymerase (New England Biolabs) and primers shown in Table S3. Plasmids were purified and analyzed by BstEII digestion (New England Biolabs) for confirmation of correct construction and electroporated into electrocompetent *E. faecalis* T11 as previously described (80). Putative electrotransformant colonies were analyzed by PCR for confirmation of acyltransferase presence and sequence-confirmed via Sanger sequencing (Massachusetts General Hospital DNA Core). Plasmids were purified using the Genjet Plasmid Miniprep MKit (Thermo Scientific). LPC (15:0) was obtained from Avanti Polar Lipids.

Crude cell extract PC assay. *E. faecalis* strains were cultured overnight in BHI with chloramphenicol. 3 mL of each culture was pelleted in a 1.5 mL microcentrifuge tube and frozen at -80°C until use. Frozen cell pellets were thawed on ice, washed with 1X PBS, resuspended in 1 mL 1X PBS, and transferred to Lysing matrix B bead-beater

tubes (MP Biomedical). Cells were homogenized using a Fast Prep 24 bead beater (MP Biomedical) for 4 x 20 sec cycles at 4.0 $m.s^{-1}$, with tubes cooling for 5 min between cycles. Immediately after the fourth cycle, 400 µL cell homogenate was added to Corning Pyrex glass tubes containing the following: 400 µL reaction mixture, modified from a previous report (81), containing (50 mM Tris-HCL pH 7.5, 0.1% Triton X-100, and 2 mM $MgCl_2$), 0.08 mg of LPC 20:0, and 0.16 mg palimtoyl-CoA (Sigma-Aldrich). Reactions were incubated at 30°C for 1 hr before lipid extractions were performed.

Growth curves. Individual colonies were incubated overnight in 5 mL DM. Cultures were diluted to a starting OD_{600nm} of 0.05 in pre-warmed 20 mL DM, DM with 130 µM GPC, and THB. OD_{600nm} was monitored every hour using a Thermo Scientific Genesys 30 spectrophotometer. Growth curves were performed in biological triplicates for each strain.

Average nucleotide identity (ANI) analysis

The ANI calculator (50, 51) was used with default parameters to analyze the following genomes: SM43, *S. oralis* ATCC 35037 (PRJNA38733) and *S. mitis* ATCC 49456 (PRJNA173).

Accession numbers

The SM43 whole genome sequence generated in this study has been deposited in Genbank under the accession number CP040231. Illumina and SMRT sequence reads

generated in this study have been deposited in the Sequence Read Archive under the accession number PRJNA542100.

Acknowledgments

This work was supported by R01AI116610, R21AI130666, and the Cecil H. and Ida Green Chair in Systems Biology Science to K.P. and GM069338 and EY023666 to Z.G. We gratefully acknowledge Dr. Michael Federle and Jennifer Chang at the University of Illinois at Chicago for providing *S. pneumoniae* cell pellets from THB+Y for our original analysis and for hosting L.J. for *S. pneumoniae* culture work.

References

1. Doern CD, Burnham CAD (2010) It's not easy being green: The viridans group streptococci, with a focus on pediatric clinical manifestations. *J Clin Microbiol* 48(11):3829–3835.

2. Mitchell J (2011) *Streptococcus mitis*: Walking the line between commensalism and pathogenesis. *Mol Oral Microbiol* 26(2):89–98.

3. Kolenbrander PE, London J (1993) Adhere today, here tomorrow: Oral bacterial adherence. *J Bacteriol* 175(11):3247–3252.

4. Murdoch DR, et al. (2009) Clinical presentation, Etiology and Outcome of Infective Endocarditis in the 21st Century: The International Collaboration on Endocarditis-Prospective Cohort Study. *Arch Intern Med* 169(5):463–473.

5. Marín M, Gudiol C, Garcia-Vidal C, Ardanuy C, Carratalà J (2014) Bloodstream infections in patients with solid tumors: Epidemiology, antibiotic therapy, and outcomes in 528 episodes in a single cancer center. *Medicine (Baltimore)* 93(3):143–149.

6. Gudiol C, et al. (2013) Changing aetiology, clinical features, antimicrobial resistance, and outcomes of bloodstream infection in neutropenic cancer patients. *Clin Microbiol Infect* 19(5):474–479.

7. Shelburne SA, et al. (2014) *Streptococcus mitis* strains causing severe clinical disease in cancer patients. *Emerg Infect Dis* 20(5):762–771.

8. Kawamura Y, Hou X-G, Sultana F, Miura H, Ezaki T (1995) Determination of 16S

rRNA Sequences of *Streptococcus mitis* and *Streptococcus gordonii* and Phylogenetic Relationships among Members of the Genus *Streptococcus*. *Int J Syst Bacteriol* 45(2):406–408.

9. Scholz CFP, Poulsen K, Kilian M (2012) Novel Molecular Method for Identification of *Streptococcus pneumoniae* Applicable to Clinical Microbiology and 16S rRNA Sequence-Based Microbiome Studies. *J Clin Microbiol* 50(6):1968–1973.

10. Kilian M, Riley DR, Jensen A, Brüggemann H, Tettelin H (2014) Parallel Evolution of *Streptococcus pneumoniae* and *Streptococcus mitis* to Pathogenic and Mutualisti Lifestyles. *MBio* 5(4):e01490-14.

11. Skov Sørensen UB, Yao K, Yang Y, Tettelin H, Kilian M (2016) Capsular Polysaccharide Expression in Commensal *Streptococcus* Species: Genetic and Antigenic Similarities to *Streptococcus pneumoniae*. *MBio* 7(6):e01844-16.

12. Jensen A, Valdórsson O, Frimodt-Møller N, Hollingshead S, Kilian M (2015) Commensal Streptococci Serve as a Reservoir for β-Lactam Resistance Genes in *Streptococcus pneumoniae*. *Antimicrob Agents Chemother* 59(6):3529–3540.

13. Shekhar S, et al. (2018) Antibodies reactive to commensal *Streptococcus mitis* show cross-reactivity with virulent *Streptococcus pneumoniae* serotypes. *Front Immunol* 9:747.

14. Adams HM, Joyce LR, Guan Z, Akins RL, Palmer KL (2017) *Streptococcus mitis* and *S. oralis* Lack a Requirement for CdsA, the Enzyme Required for Synthesis of Major Membrane Phospholipids in Bacteria. *Antimicrob Agents Chemother*

61(5):e02552-16.

15. Mishra NN, et al. (2017) Perturbations of Phosphatidate Cytidylyltransferase (CdsA) Mediate Daptomycin Resistance in *Streptococcus mitis/oralis* by a Novel Mechanism. *Antimicrob Agents Chemother* 61(4):1–13.

16. Humphries RM, Pollett S, Sakoulas G (2013) A current perspective on daptomycin for the clinical microbiologist. *Clin Microbiol Rev* 26(4):759–780.

17. Meiers M, et al. (2014) Altered lipid composition in *Streptococcus pneumoniae* cpoA mutants. *BMC Microbiol* 14(1):1–12.

18. Trombe M-C, Lanéelle M-A, Lanéelle G (1979) Lipid composition of aminopterin-resistant and sensitive strains of *Streptococcus pneumoniae*. *Biochim Biophys Acta - Lipids Lipid Metab* 574:290–300.

19. Brundish DE, Shaw N, Baddiley J (1967) The phospholipids of Pneumococcus I-192R, A.T.C.C. 12213. *Biochem J* 104:205–11.

20. Custer JE, Goddard BD, Matter SF, Kaneshiro ES (2014) The relative proportions of different lipid classes and their fatty acid compositions change with culture age in the cariogenic dental pathogen *Streptococcus mutans* UA159. *Lipids* 49:543–554.

21. Chiu T-H, Hung S-A (1979) Effect of age on the membrane composition of *Streptococcus sanguis*. *Biochim Biophys Acta* 558:267–272.

22. Goldfine H, Guan Z (2015) Lipidomic Analysis of Bacteria by Thin-Layer Chromatography and Liquid Chromatography/Mass Spectrometry. *Hydrocarbon*

and Lipid Microbiology Protocols, pp 125–139.

23. Sohlenkamp C, López-Lara IM, Geiger O (2003) Biosynthesis of phosphatidylcholine in bacteria. *Prog Lipid Res* 42:115–162.

24. Bogdanov M, Sun J, Kaback HR, Dowhan W (1996) A phospholipid acts as a chaperone in assembly of a membrane transport protein. *J Biol Chem* 271(20):11615–11618.

25. Bogdanov M, Umeda M, Dowhan W (1999) Phospholipid-assisted Refolding of an Integral Membrane Protein. *J Biol Chem* 274(18):12339–12345.

26. Lysenko ES, Gould J, Bals R, Wilson JM, Weiser JN (2000) Bacterial Phosphorylcholine Decreases Susceptibility to the Antimicrobial Peptide LL-37/hCAP18 Expressed in the Upper Respiratory Tract. *Infect Immun* 68(3):1664–1671.

27. Geiger O, López-Lara IM, Sohlenkamp C (2013) Phosphatidylcholine biosynthesis and function in bacteria. *Biochim Biophys Acta - Mol Cell Biol Lipids* 1831:503–513.

28. Conover GM, et al. (2008) Phosphatidylcholine synthesis is required for optimal function of *Legionella pneumophila* virulence determinants. *Cell Microbiol* 10(2):514–528.

29. Comerci DJ, Altabe S, De Mendoza D, Ugalde RA (2006) *Brucella abortus* synthesizes phosphatidylcholine from choline provided by the host. *J Bacteriol* 188(5):1929–1934.

30. Aktas M, Danne L, Moller P, Narberhaus F (2014) Membrane lipids in *Agrobacterium tumefaciens*: biosynthetic pathways and importance for pathogenesis. *Front Plant Sci* 5:109.

31. Aktas M, et al. (2010) Phosphatidylcholine biosynthesis and its significance in bacteria interacting with eukaryotic cells. *Eur J Cell Biol* 89(12):888–894.

32. Malek AA, Wargo MJ, Hogan DA (2012) Absence of membrane phosphatidylcholine does not affect virulence and stress tolerance phenotypes in the opportunistic pathogen *Pseudomonas aeruginosa*. *PLoS One* 7(2):e30829.

33. Kaneshiro T, Law JH (1964) Phosphatidylcholine Synthesis in *Agrobacterium tumefaciens*. *J Biol Chem* 239(6):1705–1713.

34. De Rudder KEE, Sohlenkamp C, Geiger O (1999) Plant-exuded choline is used for rhizobial membrane lipid biosynthesis by phosphatidylcholine synthase. *J Biol Chem* 274(28):20011–20016.

35. Sohlenkamp C, De Rudder KEE, Röhrs V, López-Lara IM, Geiger O (2000) Cloning and characterization of the gene for phosphatidylcholine synthase. *J Biol Chem* 275(25):18919–18925.

36. DeLong CJ, Shen Y-J, Thomas MJ, Cui Z (1999) Molecular distinction of phosphatidylcholine synthesis between the CDP-choline pathway and phosphatidylethanolamine methylation pathway. *J Biol Chem* 274(42):29683–29688.

37. Vences-Guzmán MÁ, et al. (2017) 1,2-Diacylglycerol choline phosphotransferase

catalyzes the final step in the unique *Treponema denticola* phosphatidylcholine biosynthesis pathway. *Mol Microbiol* 103(5):896–912.

38. Gisch N, et al. (2015) Lipoteichoic acid of *Streptococcus oralis* Uo5: a novel biochemical structure comprising an unusual phosphorylcholine substitution pattern compared to *Streptococcus pneumoniae*. *Sci Rep* 5:16718.

39. Bergström N, Jansson PE, Kilian M, Skov Sørensen UB (2000) Structures of two cell wall-associated polysaccharides of a *Streptococcus mitis* biovar 1 strain: A unique teichoic acid-like polysaccharide and the group O antigen which is a C-polysaccharide in common with pneumococci. *Eur J Biochem* 267(24):7147–7157.

40. Seong Seo H, Cartee RT, Pritchard DG, Nahm MH (2008) A new model of pneumococcal lipoteichoic acid structure resolves biochemical, biosynthetic, and serologic inconsistencies of the current model. *J Bacteriol* 190(7):2379–2387.

41. Denapaite D, Brückner R, Hakenbeck R, Vollmer W (2012) Biosynthesis of Teichoic Acids in *Streptococcus pneumoniae* and Closely Related Species: Lessons from Genomes. *Microb Drug Resist* 18(3):344–358.

42. Fischer W (1997) Pneumococcal lipoteichoic and teichoic acid. *Microb Drug Resist* 3(4):309–325.

43. Moser R, Aktas M, Narberhaus F (2014) Phosphatidylcholine biosynthesis in *Xanthomonas campestris* via a yeast-like acylation pathway. *Mol Microbiol* 91(4):736–750.

44. Stålberg K, Neal AC, Ronne H, Ståhl U (2008) Identification of a novel GPCAT activity and a new pathway for phosphatidylcholine biosynthesis in *S. cerevisiae* . *J Lipid Res* 49(8):1794–1806.

45. Fisher E, Almaguer C, Holic R, Griac P, Patton-vogt J (2005) Glycerophosphocholine-dependent Growth Requires Gde1p (YPL110c) and Git1p in *Saccharomyces cerevisiae*. *J Biol Chem* 280(43):36110–36117.

46. Wishart DS, et al. (2018) HMDB 4.0: The human metabolome database for 2018. *Nucleic Acids Res* 46(D1):D608–D617.

47. Guo L, et al. (2015) Plasma metabolomic profiles enhance precision medicine for volunteers of normal health. *Proc Natl Acad Sci* 112(35):E4901–E4910.

48. Głab B, et al. (2016) Cloning of glycerophosphocholine acyltransferase (GPCAT) from fungi and plants: A novel enzyme in phosphatidylcholine synthesis. *J Biol Chem* 291(48):25066–25076.

49. Akins RL, Katz BD, Monahan C, Alexander D (2015) Characterization of high-level daptomycin resistance in viridans group streptococci developed upon in vitro exposure to daptomycin. *Antimicrob Agents Chemother* 59(4):2102–2112.

50. Rodriguez-R LM, Konstantinidis KT (2016) The enveomics collection: a toolbox for specialized analyses of microbial genomes and metagenomes. *PeerJ Prepr* 4:e1900v1.

51. Goris J, et al. (2007) DNA-DNA hybridization values and their relationship to whole-genome sequence similarities. *Int J Syst Evol Microbiol* 57:81–91.

52. Rodriguez-R LM, Konstantinidis KT (2014) Bypassing Cultivation To Identify Bacterial Species. *Microbe* 9(3):111–118.

53. Konstantinidis K, Tiedje T (2005) Genomic insights that advance the species definition for prokaryotes. *PNAS* 102(7):2567–2572.

54. Ciufo S, et al. (2018) Using average nucleotide identity to improve taxonomic assignments in prokaryotic genomes at the NCBI. *Int J Syst Evol Microbiol* 68(7):2386–2392.

55. Gopalakrishnan AS, Chen Y-C, Temkin M, Dowhan W (1986) Structure and expression of the gene locus encoding the phosphatidylglycerophosphate synthase of *Escherichia coli*. *J Biol Chem* 261(3):1329–1338.

56. van Beilen J, et al. (2016) RodZ and PgsA Play Intertwined Roles in Membrane Homeostasis of *Bacillus subtilis* and Resistance to Weak Organic Acid Stress. *Front Microbiol* 7:1633.

57. Tran TT, et al. (2019) Mutations in cdsA and pgsA Correlate with Daptomycin Resistance in *Streptococcus mitis* and *S. oralis. Antimicrob Agents Chemother* 63(2). doi:10.1128/AAC.01531-18.

58. Van De Rijn I, Kessler RE (1980) Growth characteristics of group A streptococci in a new chemically defined medium. *Infect Immun* 27(2):444–448.

59. Chang JC, LaSarre B, Jimenez JC, Aggarwal C, Federle MJ (2011) Two group A streptococcal peptide pheromones act through opposing rgg regulators to control biofilm development. *PLoS Pathog* 7(8):e1002190.

60. Ojala PJ, Hirvonen TE, Hermansson M, Somerharju P, Parkkinen J (2007) Acyl chain-dependent effect of lysophosphatidylcholine on human neutrophils. *J Leukoc Biol* 82(6):1501–1509.

61. van Opijnen T, Bodi KL, Camilli A (2009) Tn-seq: high-throughput parallel sequencing for fitness and genetic interaction studies in microorganisms. *Nat Methods* 6(10):767–772.

62. Thanassi JA, Hartman-Neumann SL, Dougherty TJ, Dougherty BA, Pucci MJ (2002) Identification of 113 conserved essential genes using a high-throughput gene disruption system in *Streptococcus pneumoniae*. *Nucleic Acids Res* 30(14):3152–3162.

63. dos Santos Mota JM, Op den Kamp JAF, Verheij HM, van Deenen LL (1970) Phospholipids of *Streptococcus faecalis*. *J Bacteriol* 104(2):611–619.

64. Rashid R, et al. (2017) Comprehensive analysis of phospholipids and glycolipids in the opportunistic pathogen *Enterococcus faecalis*. *PLoS One* 12(4):e0175886.

65. Hullahalli K, Rodrigues M, Nguyen UT, Palmer K (2018) An Attenuated CRISPR-Cas System in *Enterococcus faecalis* Permits DNA Acquisition. *MBio* 9(3):e00414-18.

66. Yao J, Rock CO (2014) Phosphatidic acid synthesis in bacteria. *Biochim Biophys Acta - Mol Cell Biol Lipids* 1831(3):495–502.

67. Robertson RM, et al. (2017) A two-helix motif positions the active site of lysophosphatidic acid acyltransferase for catalysis within the membrane bilayer.

Nat Struct Mol Biol 24(8):666–671.

68. Jiang D, et al. (2014) Structural analysis of Mycobacterium tuberculosis ATP-binding cassette transporter subunit UgpB reveals specificity for glycerophosphocholine. *FEBS J* 281:331–341.

69. Großhennig S, Schmidl SR, Schmeisky G, Busse J, Stülke J (2013) Implication of glycerol and phospholipid transporters in *Mycoplasma pneumoniae* growth and virulence. *Infect Immun* 81(3):896–904.

70. Yang K, Wang M, Metcalf WW (2009) Uptake of Glycerol-2-Phosphate via the ugp-Encoded Transporter in *Escherichia coli* K-12. *J Bacteriol* 191(14):4667–4670.

71. Gupta R, Shah P, Swiatlo E (2009) Differential gene expression in *Streptococcus pneumoniae* in response to various iron sources. *Microb Pathog* 47:101–109.

72. Clinical and Laboratory Standards Institute (2016) *Performance standards for antimicrobial susceptibility testing, 26th ed. CLSI supplement M100S*.

73. Wick RR, Judd LM, Gorrie CL, Holt KE (2017) Unicycler: Resolving bacterial genome assemblies from short and long sequencing reads. *PLoS Comput Biol* 13(6):e1005595.

74. Morrison DA, Khan R, Junges R, Åmdal HA, Petersen FC (2015) Genome editing by natural genetic transformation in *Streptococcus mutans*. *J Microbiol Methods* 119:134–141.

75. Salvadori G, Junges R, Morrison DA, Petersen FC (2016) Overcoming the barrier

of low efficiency during genetic transformation of *Streptococcus mitis*. *Front Microbiol* 7:1009.

76. Biswas I, Gruss A, Ehrlich SD, Maguin E (1993) High-efficiency gene inactivation and replacement system for gram-positive bacteria. *J Bacteriol* 175(11):3628–3635.

77. Tan BK, et al. (2012) Discovery of a cardiolipin synthase utilizing phosphatidylethanolamine and phosphatidylglycerol as substrates. *Proc Natl Acad Sci* 109(41):16504–16509.

78. Li C, Tan BK, Zhao J, Guan Z (2016) In vivo and in vitro synthesis of phosphatidylglycerol by an *Escherichia coli* cardiolipin synthase. *J Biol Chem* 291(48):25144–25153.

79. Lu W, Kimball E, Rabinowitz JD (2006) A high-performance liquid chromatography-tandem mass spectrometry method for quantitation of nitrogen-containing intracellular metabolites. *J Am Soc Mass Spectrom* 17:37–50.

80. Bae T, Kozlowicz B, Dunny GM (2002) Two targets in pCF10 DNA for PrgX binding: Their role in production of Qa and prgX mRNA and in regulation of pheromone-inducible conjugation. *J Mol Biol* 315:995–1007.

81. Chang YY, Kennedy EP (1967) Phosphatidyl glycerophosphate phosphatase. *J Lipid Res* 8:456–62.

Figures

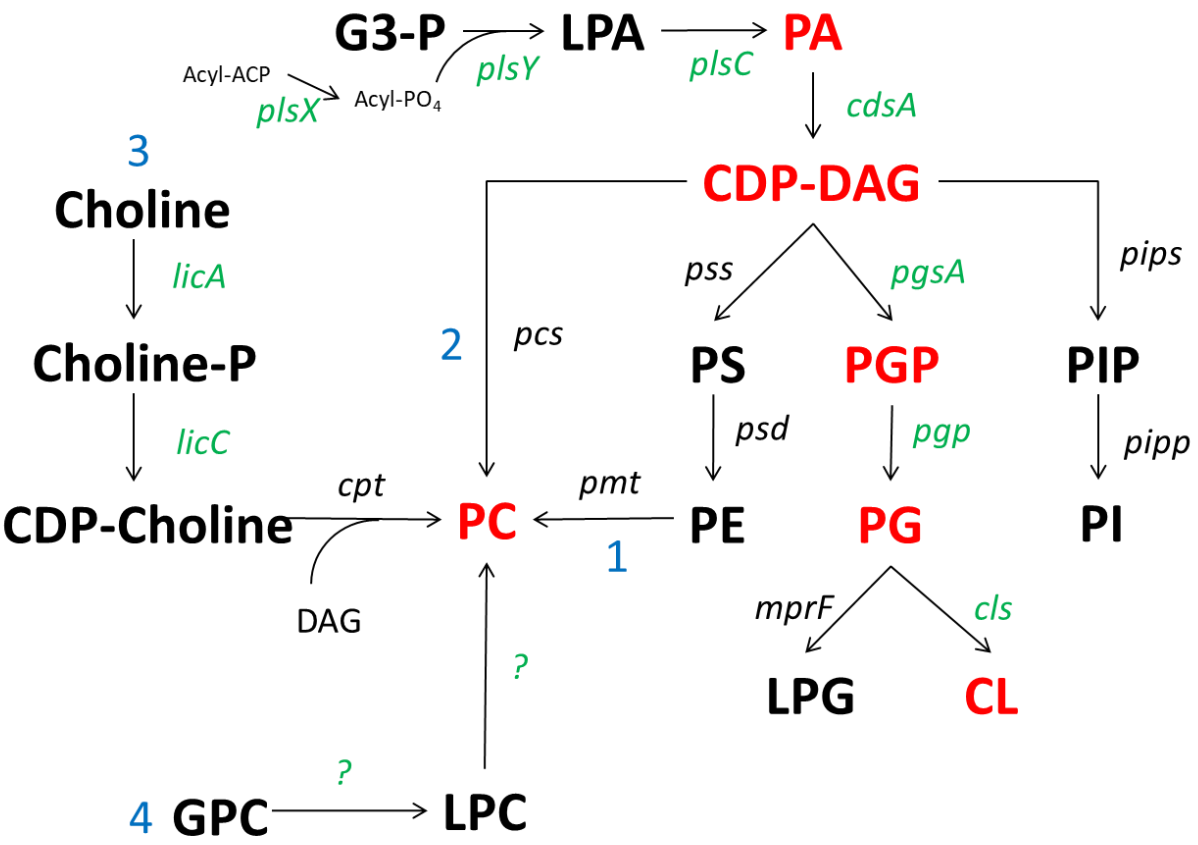

Figure 1. Phospholipid pathways in bacteria, including pathways for PC biosynthesis. Shown are the methylation pathway (1), phosphatidylcholine synthase pathway (2), CDP-choline pathway (3), and the glycerophosphocholine pathway (4). Lipids detected in THB-cultured SM43 are shown in red. Genes encoded by SM43 are shown in green. Abbreviations are PA, phosphatidic acid; CDP-DAG, CDP-diacylglycerol; PS, phosphatidylserine; PE, phosphatidylethanolamine; G3-P, glycerol-3-phosphate; PGP, phosphatidylglycerol-3-P; PG, phosphatidylglycerol; CL, cardiolipin; LPG, lysly-phosphatidylglycerol; PIP, phosphatidylinositolphosphate; PI,

phosphatidylinosotiol; PC, phosphatidylcholine, LPC, lysophosphatidylcholine; GPC, glycerophosphocholine; LPA, lysophosphatidic acid.

Table 1. Summary of major glycolipids and phospholipids detected in Mitis group streptococci in routine laboratory media[1].

Streptococcal species	Strain	Source	DAG	MHDAG	DHDAG	PA	PG	CL	C55-P	PC	L-PG	Growth medium[2]
S. mitis	ATCC 49456	Type strain	+	+	+	+	+	+	+	+	–	THB
S. oralis	ATCC 35037	Type strain	+	+	+	+	+	+	+	+	–	THB
	1647[3]	Endocarditis	+	+	+	+	+	+	+	+	–	THB
	1648[3]	Endocarditis	+	+	+	+	+	+	+	+	–	THB
S. pneumoniae	D39	Historical strain	+	+	+	+	+	+	+	+	–	THB+Y
	TIGR4	Bacteremia	+	+	+	+	+	+	+	+	–	THB+Y
Mitis group	1643 (SM43)[3]	Endocarditis	+	+	+	+	+	+	+	+	–	THB
	SM43Δ*cdsA*	This study	+	+	+	+	-	-	+	+	–	THB
	SM43Δ*pgsA*	This study	+	+	+	+	-	-	+	+	–	THB

[1]Abbreviations: DAG, diacylglycerol; MHDAG, monohexosyldiacylglycerol; DHDAG, dihexosyldiacylglycerol; PA, phosphatidic acid; PG, phosphatidylglycerol; CL, cardiolipin; C55-P, undecaprenyl phosphate; PC, phosphatidylcholine; L-PG, lysyl-phosphatidylglycerol
[2]Todd-Hewitt Broth (THB); THB supplemented with 0.5% yeast extract (THB+Y).
[3]Lipid profiles previously published by Adams *et al* 2017 (14).

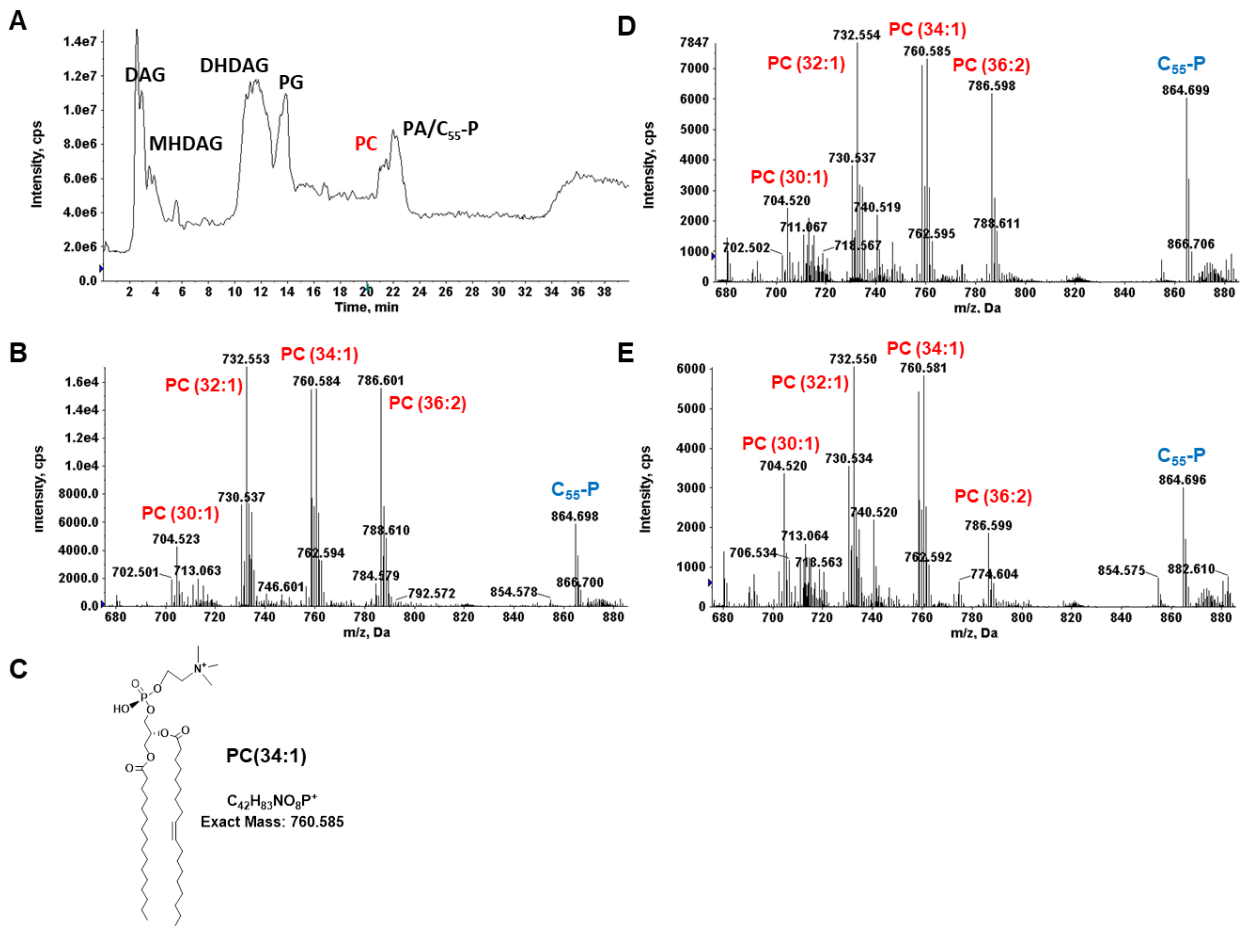

806

807 **Figure 2. PC species detected in SM43, SM43Δ*cdsA* and SM43Δ*pgsA*.** Shown are
808 the positive mode total ion chromatogram of SM43 lipids (A), the ESI-MS of SM43 PC
809 species (B), chemical structure of PC (34:1) (C), the ESI-MS of PC species in
810 SM43Δ*cdsA* (D), and E) the ESI-MS of PC species in SM43Δ*pgsA*. The mass spectra
811 shown are averaged from spectra acquired by NPLC-ESI/MS during the 20–21 min
812 window. PC species are detected by positive ion ESI/MS as the M^+ ions.

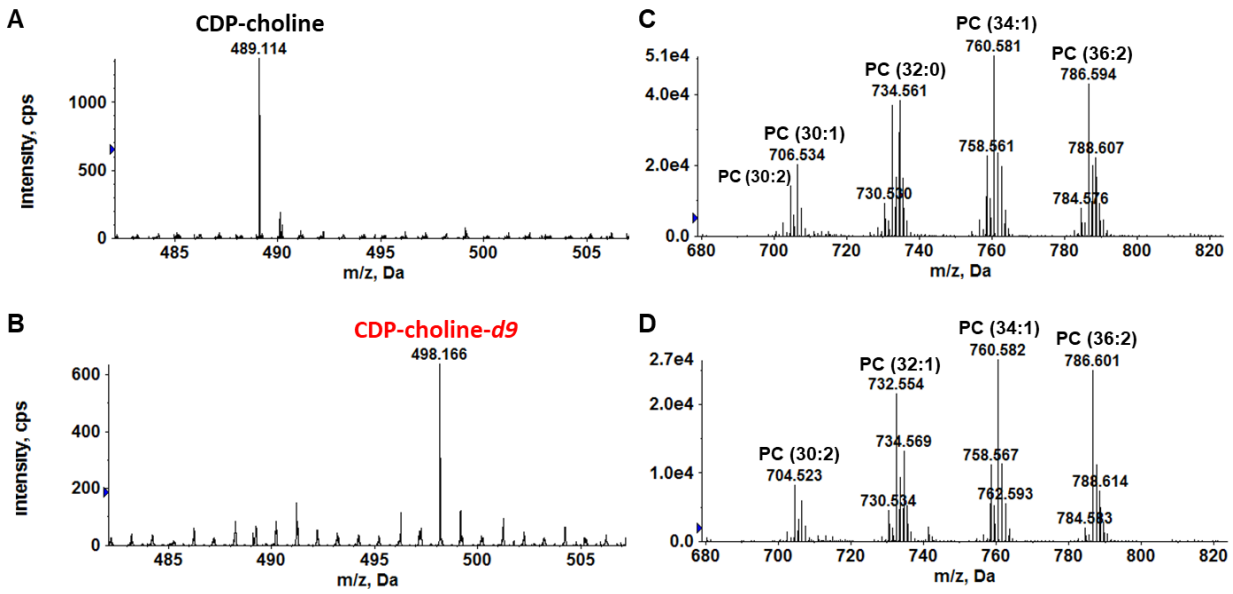

Figure 3. Exogenous deuterated choline (choline-*d9*) is used by SM43 to synthesize CDP-choline, but not PC. CDP-choline and PC were detected in the soluble-metabolite extract and lipid extract, respectively. Soluble metabolites were analyzed by reverse phase LC/ESI-MS in positive ion mode. Lipids were analyzed by normal phase LC/ESI-MS in positive ion mode. Shown are CDP-choline (M^+ ion at *m/z* 489.1) present in SM43 cultured in THB (A), and CDP-choline-*d9* (M^+ ion at *m/z* 498.1) present in SM43 cultured in THB supplemented with 2 mM choline-*d9* (B). Note the expected mass shift (9 Da) between CDP-choline and CDP-choline-*d9.* Also shown are PC species detected in SM43 cultured in THB (C), and PC species detected in SM43 cultured in THB supplemented with choline-*d9* (D). No corresponding mass shift (9 Da) is detected in the PC species, excluding the possibility of SM43 using the CDP-choline pathway for PC synthesis.

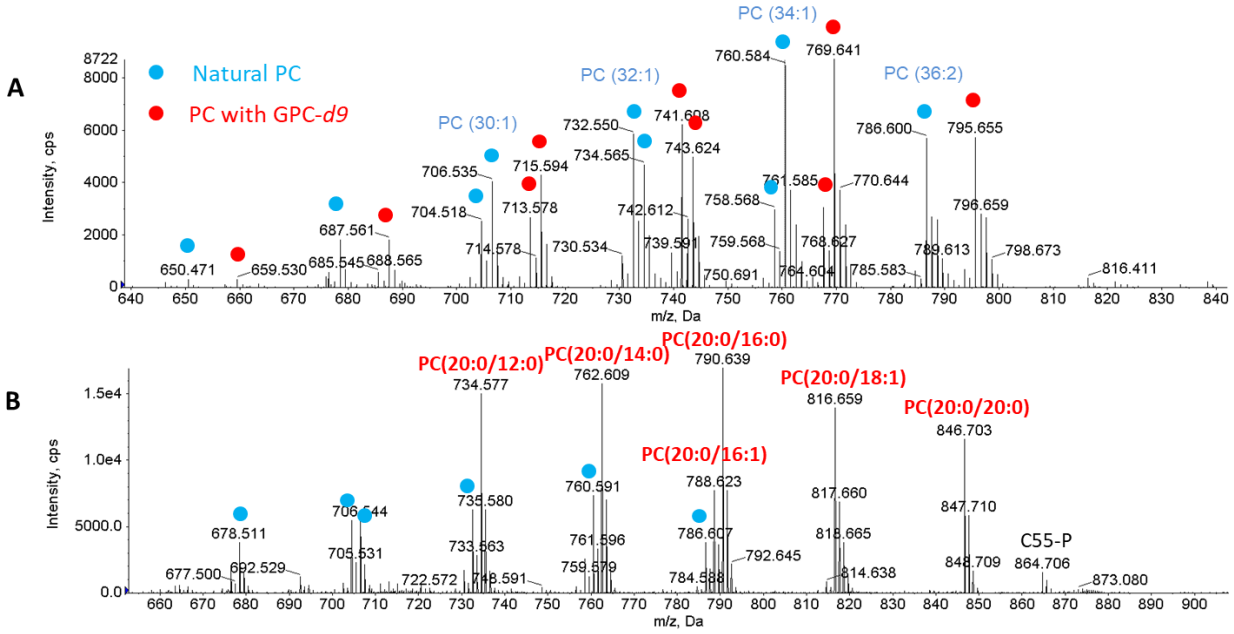

826

827 **Figure 4. PC species of SM43 cultured in THB supplemented with GPC-*d9* and**
828 **LPC (20:0).** A) ESI/MS detection of PC species in SM43 cultured with GPC-*d9*. Blue
829 dots indicate PC species normally detected in THB-grown SM43, and red dots indicate
830 GPC-*d9*-originating PC species. B) ESI/MS detection of PC species in SM43 when
831 cultured in the presence of LPC (20:0). Blue dots indicate PC species normally detected
832 in THB-grown SM43. Red dots are LPC (20:0)-originating species. Incorporation of
833 GPC-*d9* and LPC (20:0) into PC indicates that the GPC pathway is utilized by SM43 for
834 PC biosynthesis.

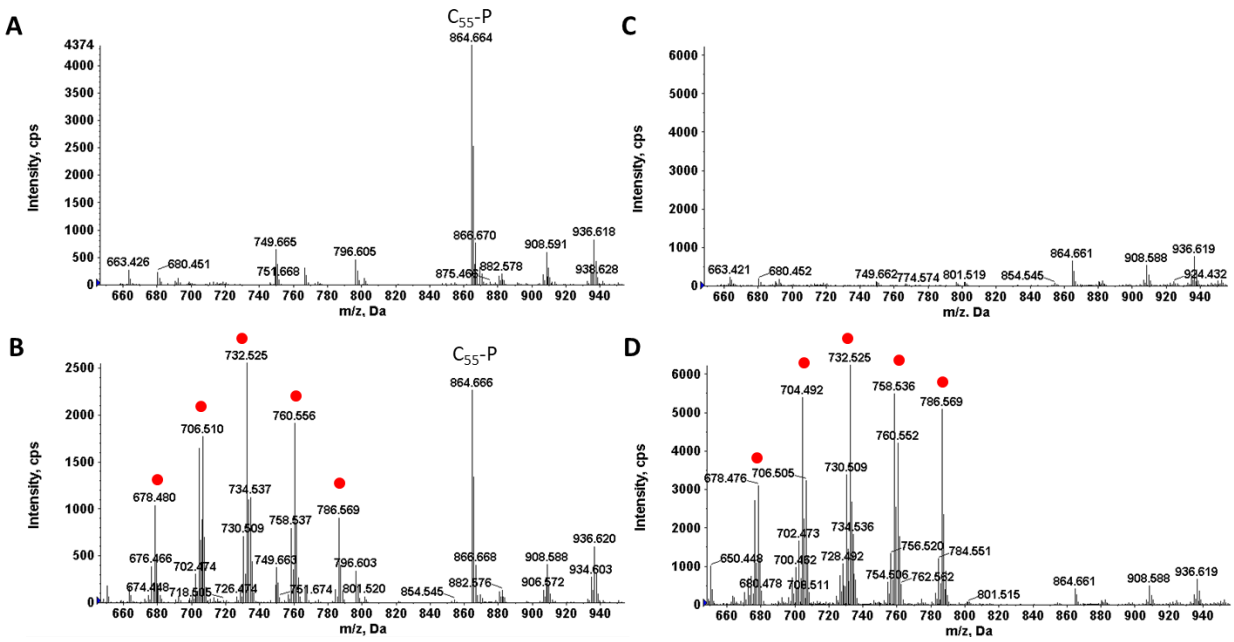

Figure 5. PC species of SM43 and *S. mitis* ATCC 49456 cultured in defined media (DM) with and without GPC. PC species (red dots) detected in SM43 (A) and ATCC 49456 (C) cultured in DM, and SM43 (B) and ATCC 49456 (D) cultured in DM supplemented with GPC are shown. PC is only detected when GPC is present in the culture medium.

Table 2. Summary of major glycolipids and phospholipids detected in Mitis group streptococci cultured in DM with or without GPC[1].

Streptococcal species	Strain	Source	DAG	MHDAG	DHDAG	PA	PG	CL	C55-P	PC	L-PG	Growth medium[2]
S. mitis	ATCC 49456	Type strain	+	+	+	+	+	+	+	-	−	DM
	ATCC 49456		+	+	+	+	+	+	+	+	−	DM+GPC
S. oralis	ATCC 35037	Type strain	+	+	+	+	+	+	+	-	−	DM
	ATCC 35037		+	+	+	+	+	+	+	+	−	DM+GPC
S. pneumoniae	D39	Historical strain	+	+	+	+	+	+	+	-	−	DM
	D39		+	+	+	+	+	+	+	+	−	DM+GPC
	TIGR4	Bacteremia	+	+	+	+	+	+	+	-	−	DM
	TIGR4		+	+	+	+	+	+	+	+	−	DM+GPC
Mitis group	1643 (SM43)	Endocarditis	+	+	+	+	+	+	+	-	−	DM
	1643 (SM43)		+	+	+	+	+	+	+	+	−	DM+GPC

[1]Abbreviations: DAG, diacylglycerol; MHDAG, monohexosyldiacylglycerol; DHDAG, dihexosyldiacylglycerol; PA, phosphatidic acid; PG, phosphatidylglycerol; CL, cardiolipin; C55-P, undecaprenyl phosphate; PC, phosphatidylcholine; L-PG, lysyl-phosphatidylglycerol

[2]Defined media (DM); Defined media supplemented with glycerophosphocholine (DM+GPC).

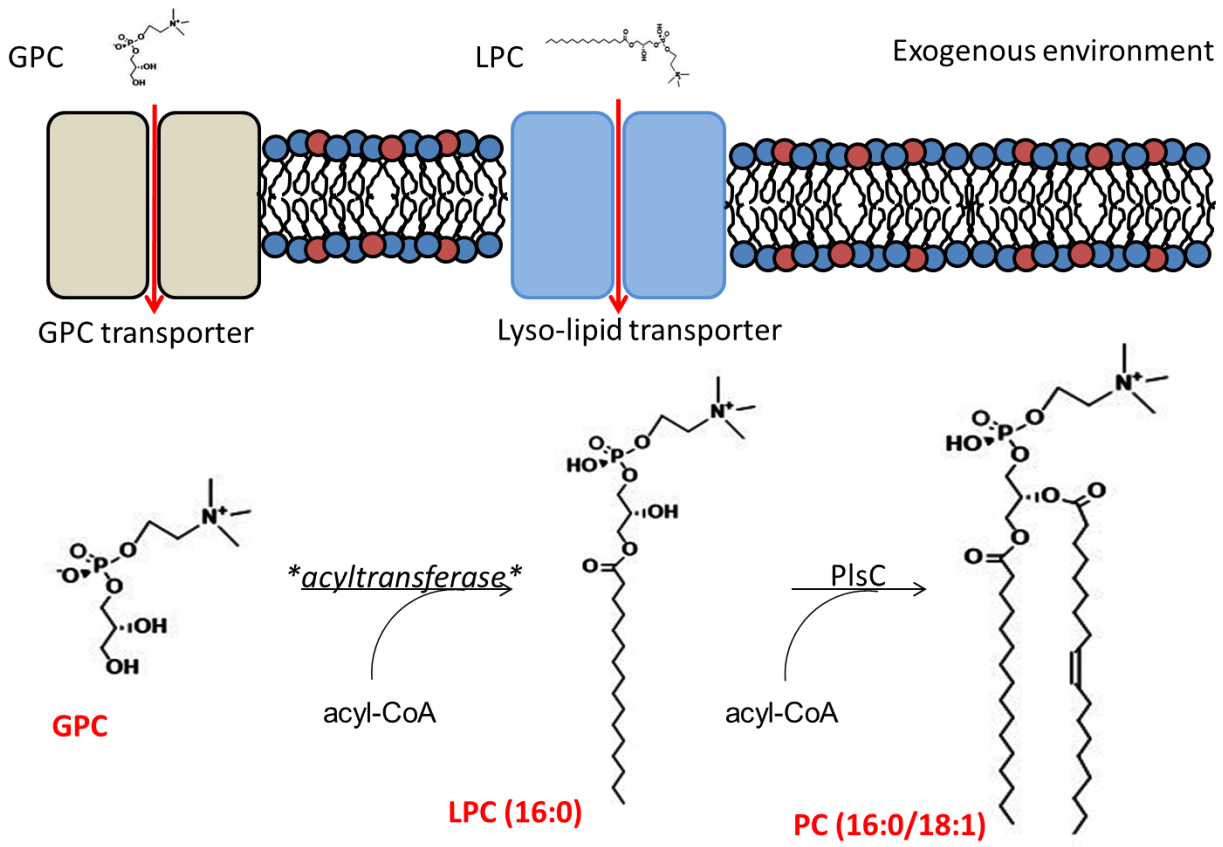

Figure 6. Proposed model for the GPC pathway in Mitis group streptococci. Exogenous GPC and LPC are transported into the cell via unidentified transporters. GPC is acylated to form LPC, and a second acylation occurs via PlsC to form PC. Acyl chain lengths vary in the lipid membrane; representative chain lengths are shown.

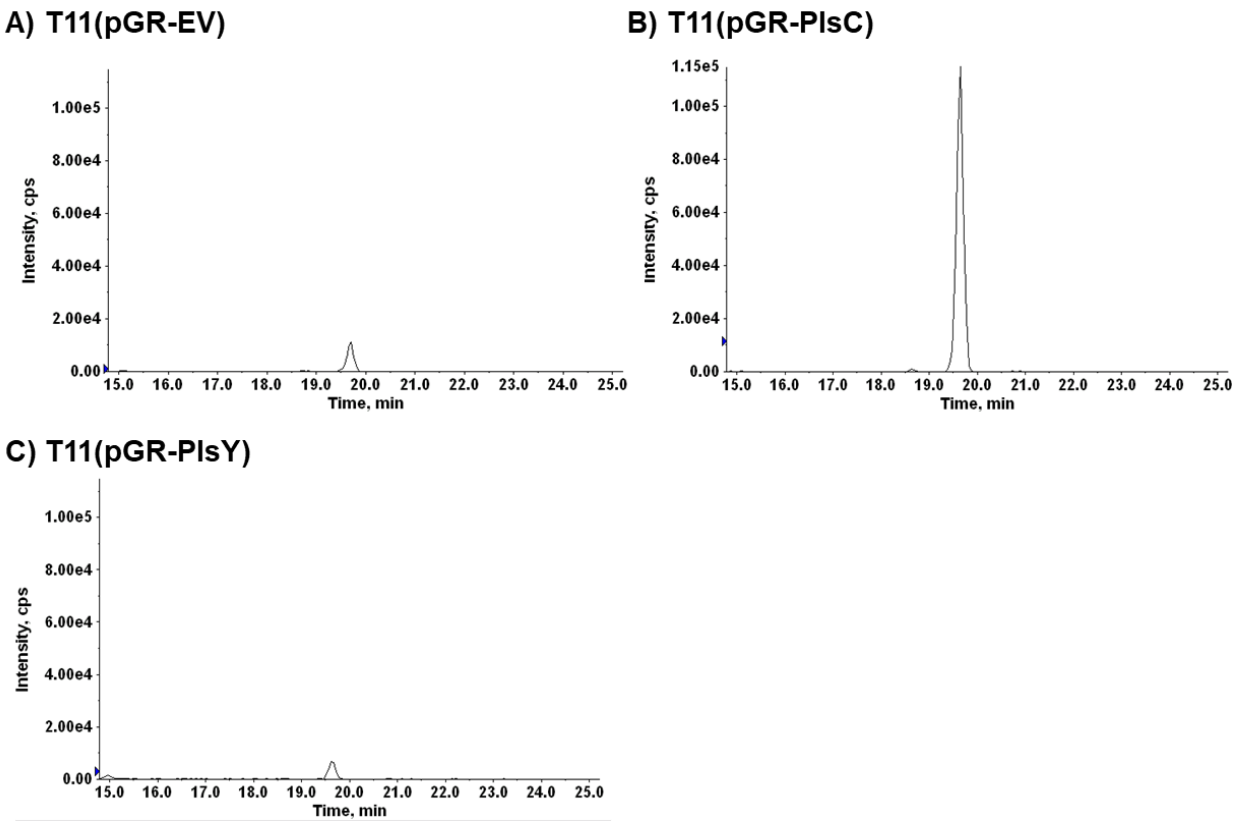

Figure 7. Heterologous expression of SM43 acyltransferases in *E. faecalis*. Extracted ion chromatograms (XIC) of PC 20:0/16:0 products from *in vitro* acyltransferase assays are shown for *E. faecalis* T11(pGR-EV) (empty vector; A), T11(pGR-PlsC) (B), and T11(pGR-PlsY) (C). Only when SM43 PlsC is expressed is a significant level of PC 20:0/16:0 generated, indicating acylation of LPC to PC activity by SM43 PlsC.

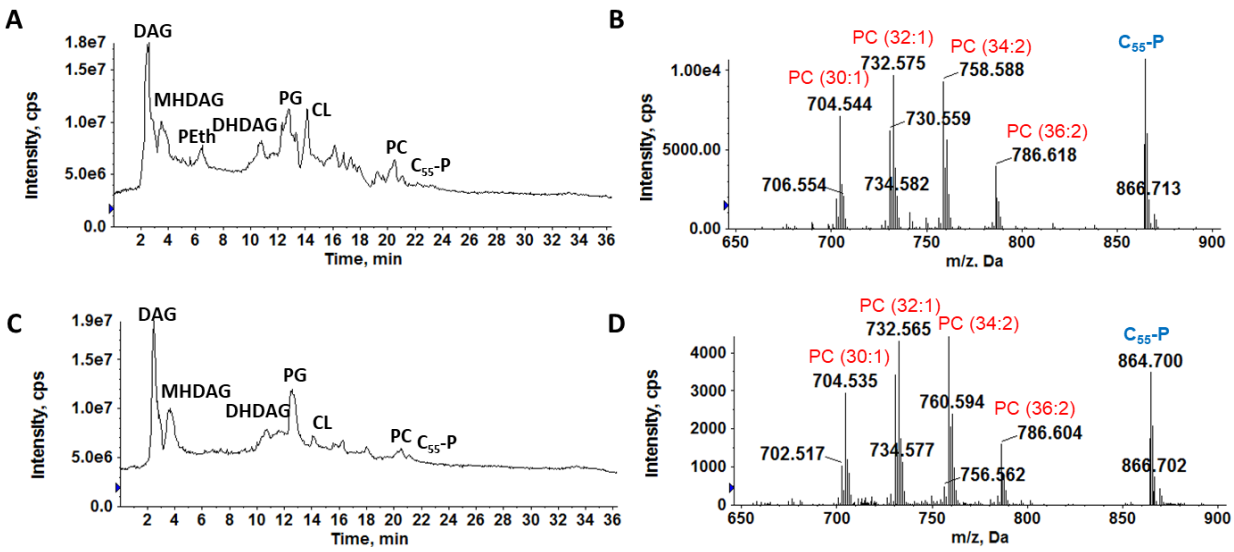

Figure 8. Positive ion total ion chromatogram (TIC) and PC mass spectrum of *S. pneumoniae* D39 and TIGR4 strains in early stationary phase. Shown are the TIC of *S. pneumoniae* D39 lipids (A), the ESI/MS of major PC species in *S. pneumoniae* D39 (B), the TIC of *S. pneumoniae* TIGR4 lipids (C), and the ESI/MS of major PC species in *S. pneumoniae* TIGR4 (D). The mass spectra shown are averaged from spectra acquired by NPLC-ESI/MS during the 19.5 – 21 min window. PC species are detected by positive ion ESI/MS as the M^+ ions, while the co-eluting undecaprenyl phosphate (C_{55}-P) is detected as the $[M+NH_4]^+$ ion (*m/z* 864.7).

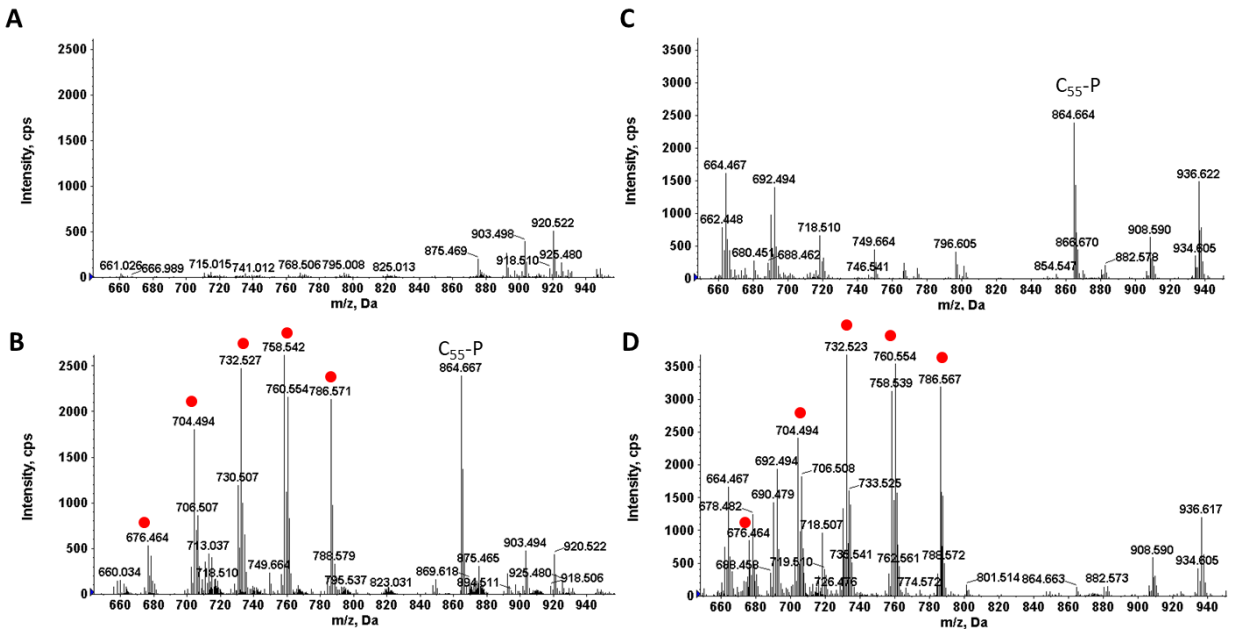

Figure 9. GPC pathway confirmation in *S. pneumoniae* D39 and *S. oralis* ATCC 35037. Shown are PC species (red dots) detected for D39 (A) and ATCC 35037 (C) cultured in DM and D39 (B) and ATCC 35037 (D) cultured in DM supplemented with GPC. PC is only detected when GPC is present in the culture medium.

Phosphatidylcholine biosynthesis in Mitis group streptococci via a host metabolite scavenging pathway

Supplemental information

Supplemental information

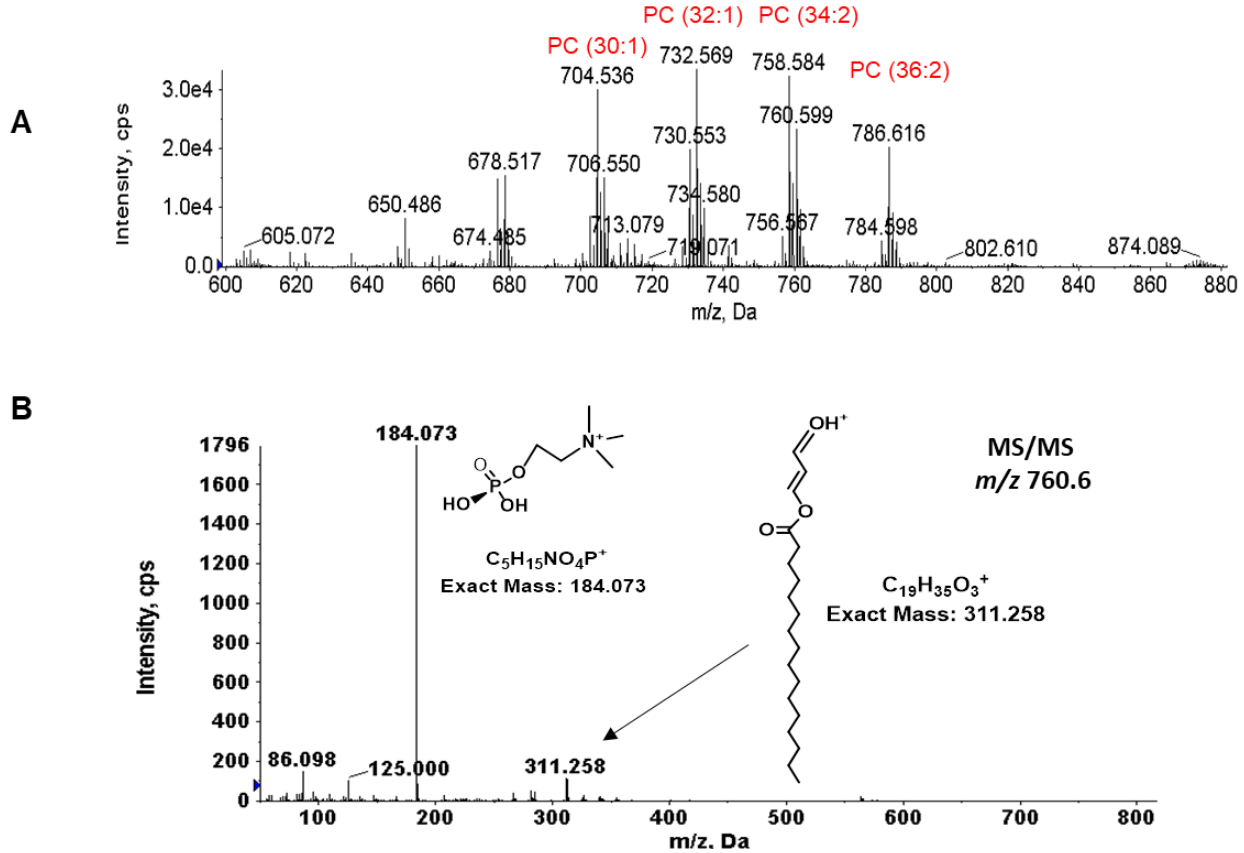

Supplemental Figure 1. Phosphatidylcholine (PC) species in *S. mitis* ATCC 49456. A) *S. mitis* ATCC 49456, B) MS/MS daughter ion fragmentation of PC (34:1) *m/z* 760.6 in SM43. The mass spectra shown are averaged from spectra acquired by NPLC-ESI/MS during the 20–21 min window. PC species are detected by positive ion ESI/MS as the M^+ ions.

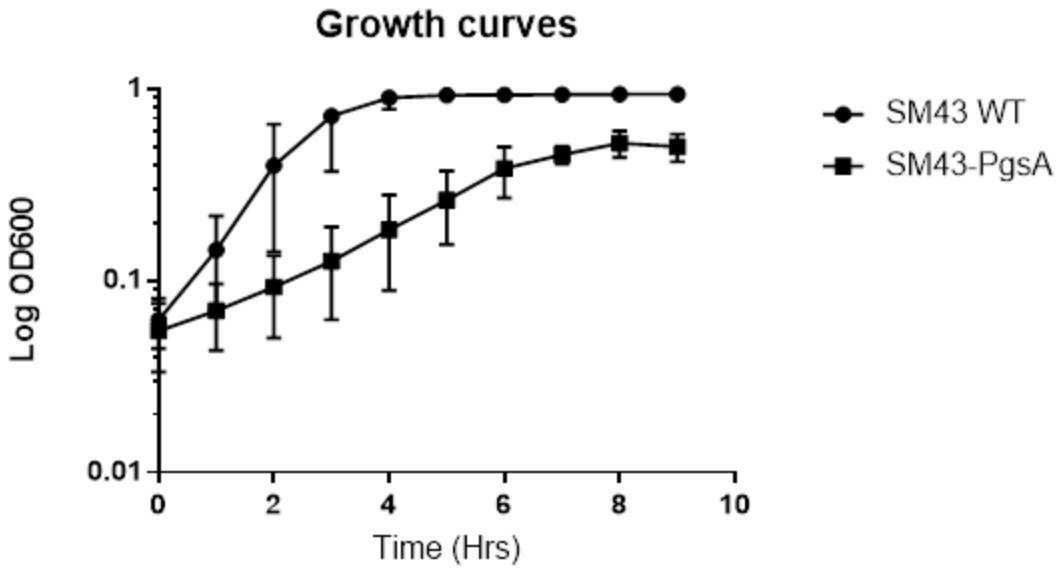

886

887 **Supplemental Figure 2**. **Growth curves.** Shown are growth curves for SM43 and
888 SM43Δ*pgsA* in THB. OD_{600nm} readings were taken every hour, with a starting inoculum
889 of OD_{600} 0.05. Growth curve was performed as biological triplicate. Error bars indicate
890 standard deviation.

891 **Supplemental Table 1. Daptomycin susceptibility data.**

Strain	Dap MIC (µg/mL)
SM43	<1
SM43Δ*pgsA*	>256
SM43Δ*cdsA*	>256

892

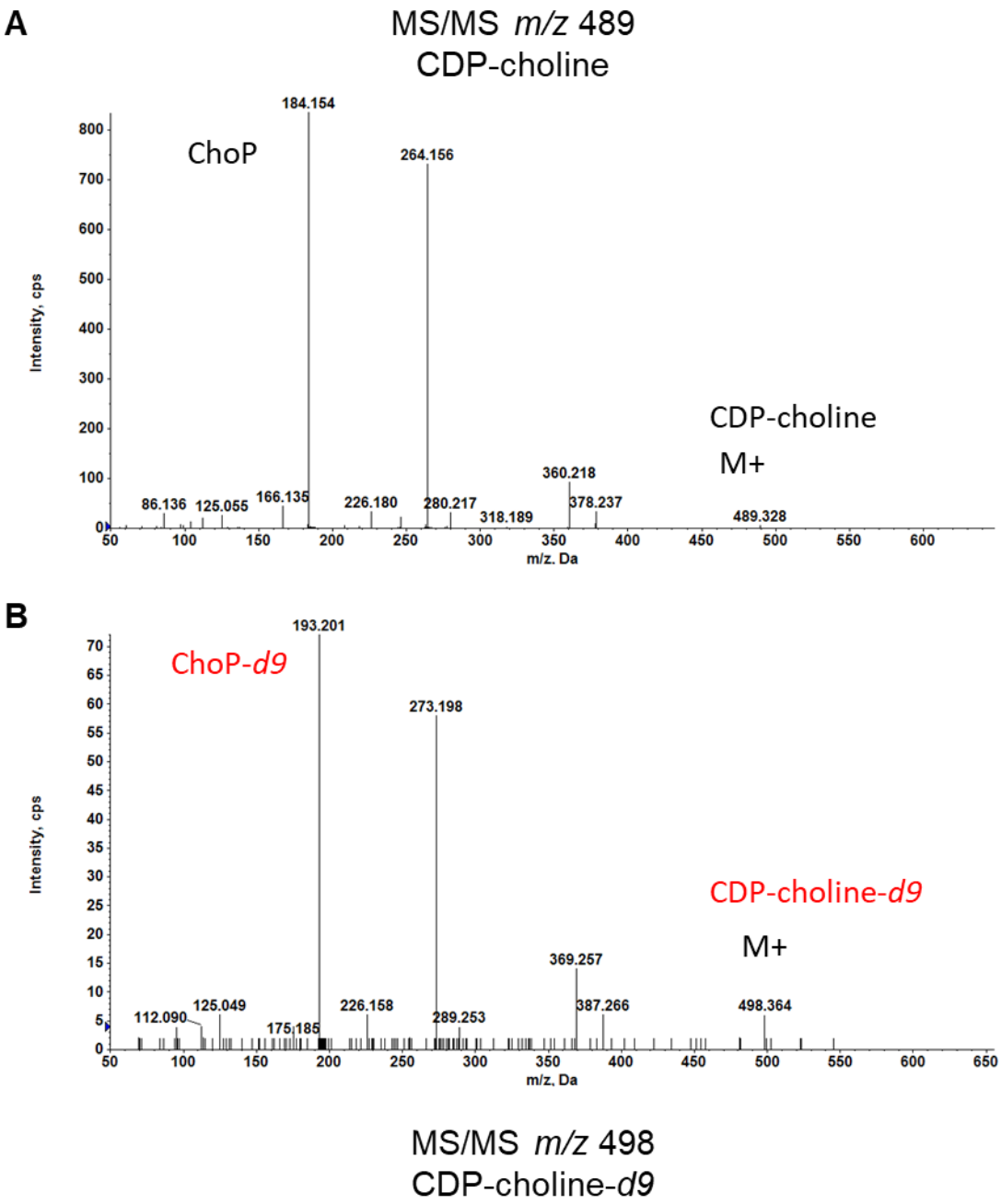

Supplemental Figure 3. MS/MS fragmentation of CDP-choline and CDP-choline-*d9*. A) MS/MS of CDP-choline (*m/z* 489) B) MS/MS of CDP-choline-*d9* (*m/z* 498). Note the mass shift of 9-*da* for all major MS/MS peaks in B.

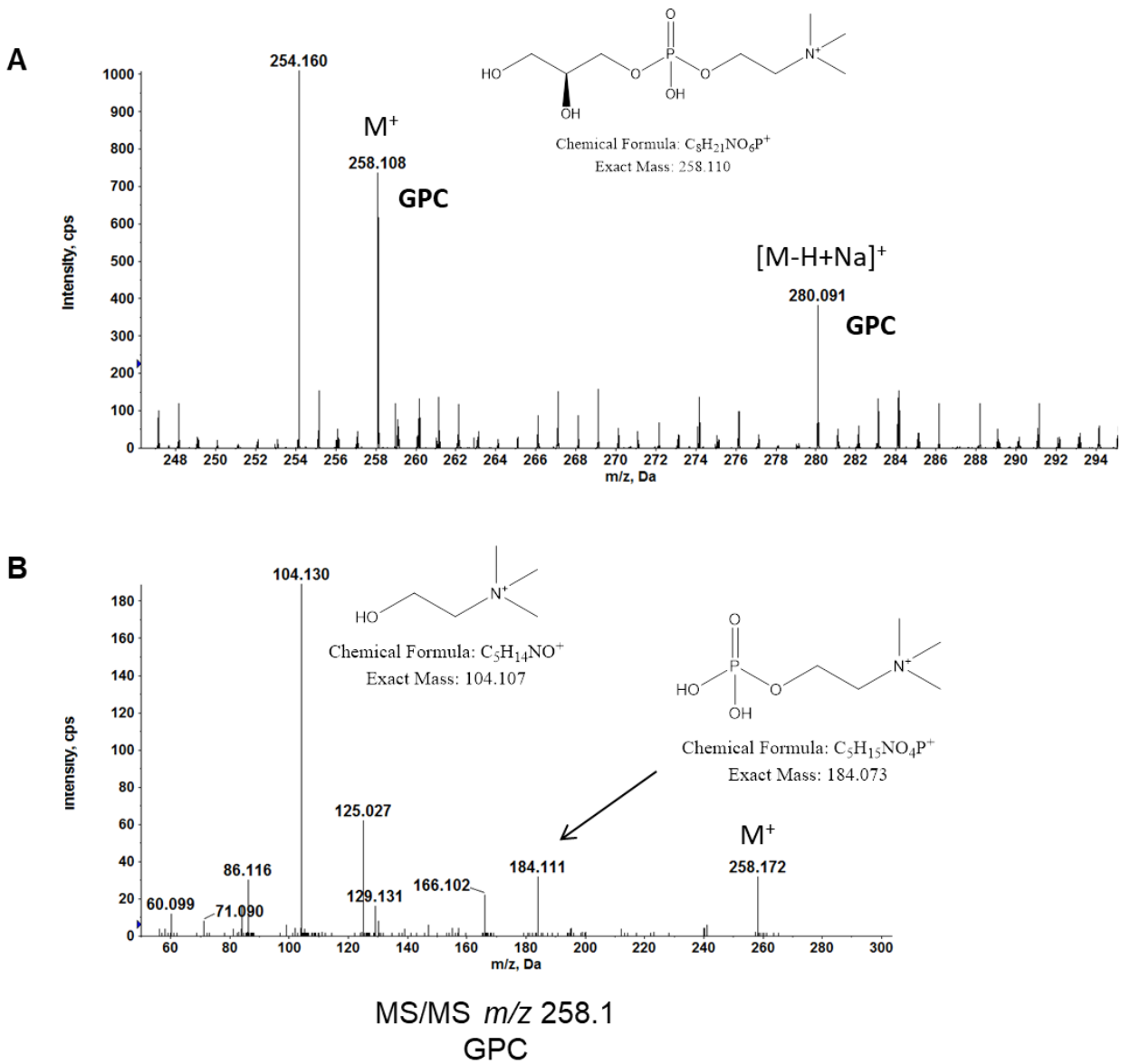

Supplemental Figure 4. MS detection of GPC in THB. The soluble-metabolite extract of THB was analyzed by reverse phase LC/MS. A) GPC is detected by positive ion ESI/MS as the M^+ ion at *m/z* 258.108 and $[M-H+Na]^+$ ion at *m/z* 280.091. B) MS/MS spectrum of the M^+ ion (*m/z* 258.1) of GPC. The chemical structures of major fragments are shown.

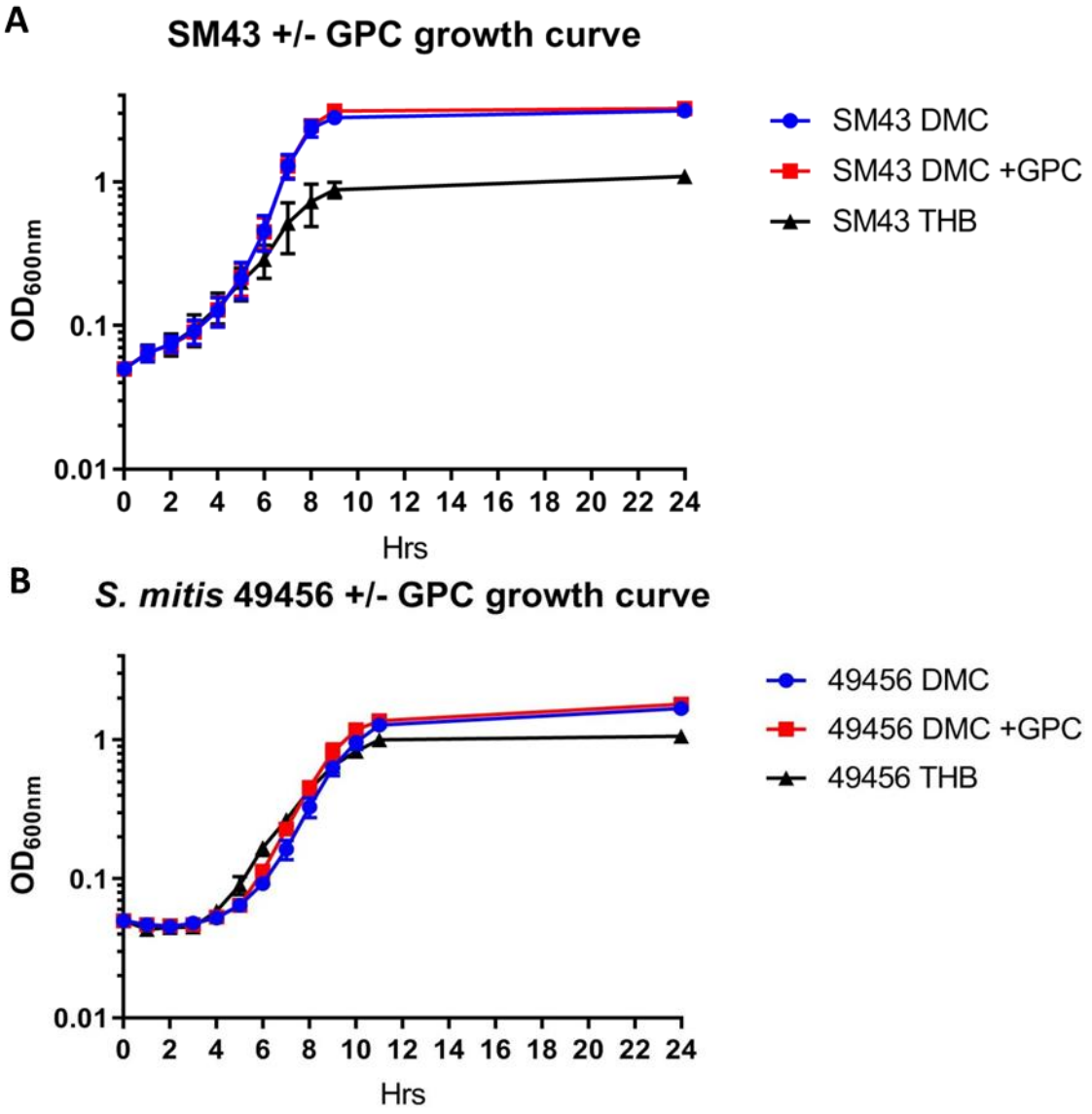

903

904 **Supplemental Figure 5. Growth curves of SM43 (A) and ATCC 49456 (B) in THB,**
905 **and in defined medium (DM) with and without GPC supplementation.** Growth
906 curves were done in biological triplicates.

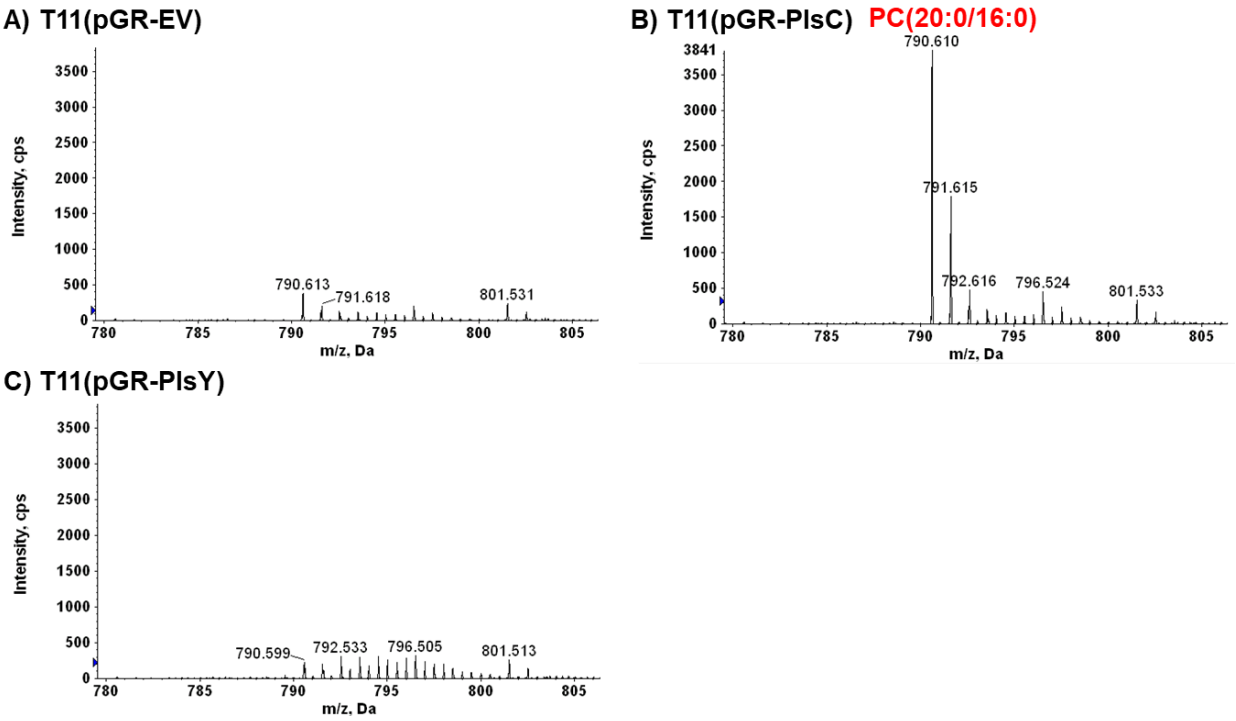

907

908 **Supplemental Figure 6. ESI/MS of PC 20:0/16:0 in heterologous host expression**
909 **assay.** Shown are A) *E. faecalis* T11(pGR-EV) (empty vector), B) T11(pGR-PlsC), and
910 C) T11(pGR-PlsY). The mass spectra shown are averaged from spectra acquired by
911 NPLC-ESI/MS during the 19–20 min window. PC species are detected by positive ion
912 ESI/MS as the M^+ ions.

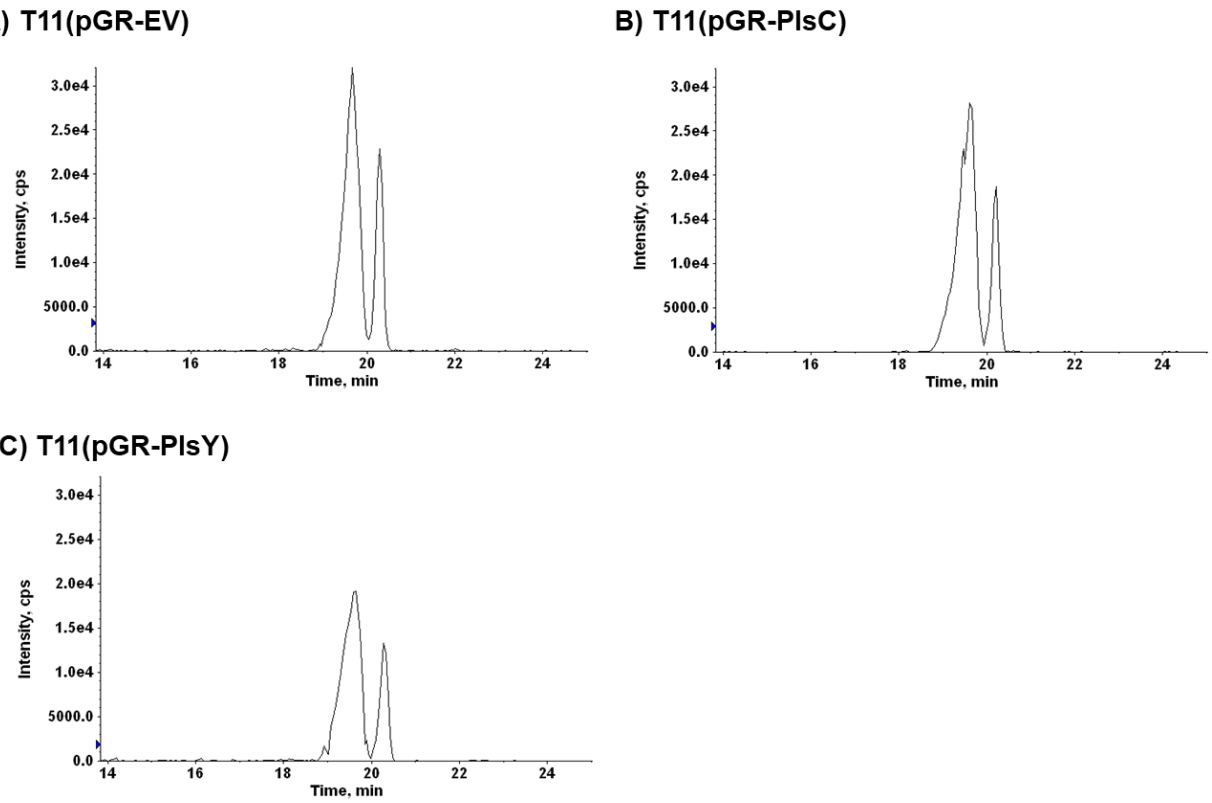

Supplemental Figure 7. Extracted ion chromatograms of lysyl-phosphatidylglycerol in heterologous host expression assay. Shown are A) *E. faecalis* T11(pGR-EV) (empty vector), B) T11(pGR-PlsC), and C) T11(pGR-PlsY). XIC's of L-PG (*m/z* 891), co-eluting with PC (20:0/16:0) present during the acyltransferase assay in Figure 7. The relative levels of L-PG are an indication of the cell mass during the assay.

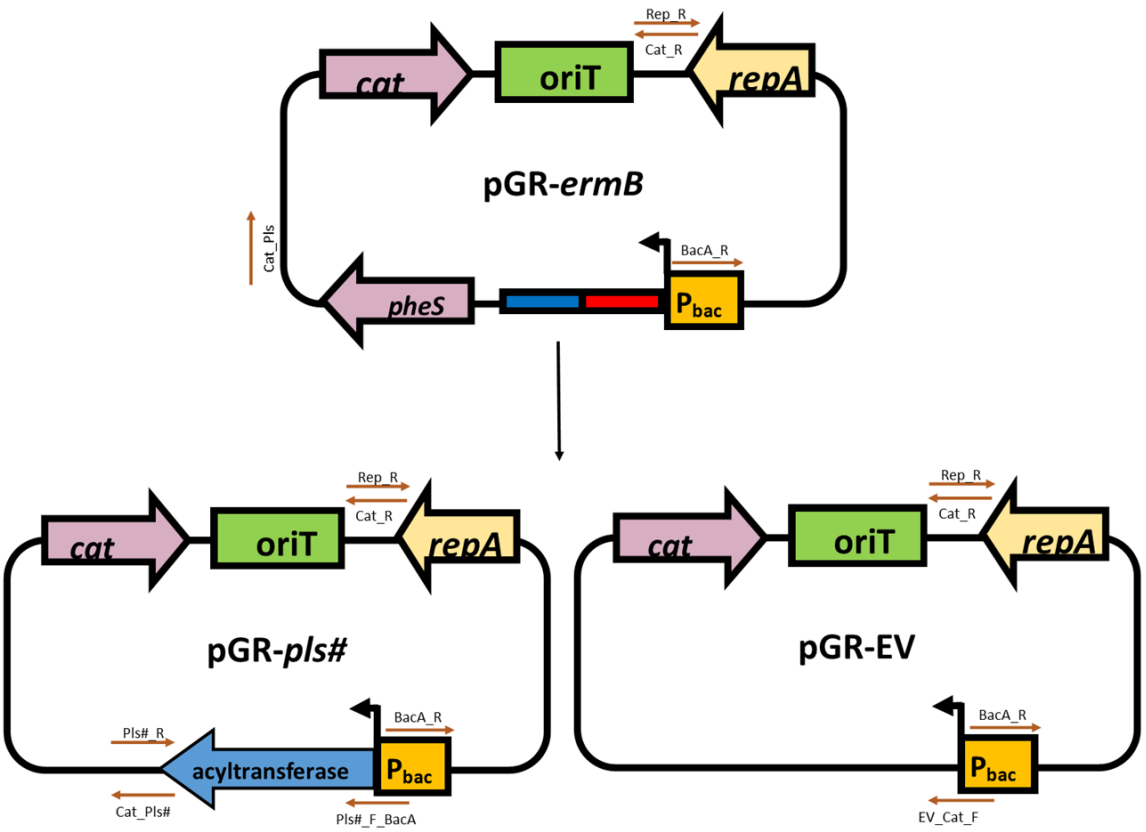

920

921 **Supplemental Figure 8. Expression vector assembly.** Primer pairs are indicated to
922 show the 3 fragments utilized for Gibson assembly of the acyltransferase expression
923 vectors.

Table S2. Strains and plasmids used in this study.

Organism	Strain	Description	Ref
Mitis group streptococci	1643 (SM43)	Wild-type infective endocarditis isolate	(1)
	1643Δ*cdsA*	*cdsA* deletion strain	This work
	1643Δ*pgsA::ermB*	*pgsA* deletion strain, replaced with *ermB*. Erm^r	This work
S. mitis	ATCC 49456 (NCTC 12261)	Wild-type *S. mitis* type strain from ATCC	(2)
S. oralis	ATCC 35037 (NCTC 11427)	Wild-type *S. oralis* type strain from ATCC	(3)
S. pneumoniae	D39	Wild type, historical strain	(4)
	TIGR4	Wild type, bloodstream isolate	(5)
E. faecalis	T11	Urine isolate, wild type strain	(6)
	T11(pGR-EV)	Empty vector control	This work
	T11(pGR-PlsY)	Expresses SM43 *plsY* from P_{bacA}	This work
	T11(pGR-PlsC)	Expresses SM43 *plsC* from P_{bacA}	This work
E. coli	DH5α	Plasmid cloning host; F^-, φ80*lac*ZΔM15, *rec*A1, *end*A1, *hsd*R17, *pho*A, *sup*E4 4, λ^- *thi*-1, *gyr*A96, *rel*A1	(7)
	DH5α(pGR-EV)	Empty vector control	This work
	DH5α(pGR-PlsY)	Expresses SM43 *plsY* from P_{bacA}	This work
	DH5α(pGR-PlsC)	Expresses SM43 *plsC* from P_{bacA}	This work
Plasmids	**Description**		**Ref**
pG^+host 4	Encodes *ermB*		(8)
pGR-*ermB*	Constitutive expression vector for *E. faecalis* with the short P_{bacA} promoter. Confers chloramphenicol resistance. Genbank Accession: MF948287		(9)
pGR-EV	pGR-*ermB* without the *ermB* spacer and with full P_{bacA}, Empty vector control		This work
pGR-PlsY	pGR-EV expressing SM43 *plsY* from P_{bacA}		This work
pGR-PlsC	pGR-EV expressing SM43 *plsC* from P_{bacA}		This work

Table S3. Primers used in this study.

Primer	Sequence (5'-3')	Use
L_Updel_F	TTTACGTGAATATATCGGT	SM43 upstream of *cdsA* region amplification
L_Updel_R PstI	ACGTCACTGCAGATCCTTGGTCATATCTTCTC	SM43 upstream of *cdsA* region amplification
L_Dwndel_F PstI	ACGTCACTGCAGCCAATGATGCACTTATTC	SM43 downstream of *cdsA* region amplification
L_Dwndel_R	CTTGATTTCTTCTTGCAC	SM43 downstream of *cdsA* region amplification
L1_R	CGTACATATCTTCGACTGTC	*cdsA* knockout sequencing with L_Updel_F
L2_F	CCTTCGTACCATGATTGAG	*cdsA* knockout sequencing
L2_R	GTCAGATTTTCCCATTTTTC	*cdsA* knockout sequencing
L3_F	TTTAGAGAATGAGGACCG	*cdsA* knockout sequencing
L3_R	CATATCTTCTGTGATGT	*cdsA* knockout sequencing
L4_F	ATGGTGGTCGTGCTGAA	*cdsA* knockout sequencing
L4_R	GATACTGTACATCCAAAGG	*cdsA* knockout sequencing
L5_F	CAGTAGATCACGATGCAAC	*cdsA* knockout sequencing
L5_R	GTCGCATAATGTCATTCC	*cdsA* knockout sequencing
L6_F	GTGTAGTTATCATGGTTG	*cdsA* knockout sequencing with L_Dwndel_R
L7F	CAAACGGCTCTTCCTATGC	*cdsA* knockout sequencing
L7R	CTGATAACTTGAGCATCG	*cdsA* knockout sequencing
SM43cdsA_reseq_F	TCAGGTCTATATGCATCTG	*cdsA* upstream resequence
SM43cdsA_reseq_R	GCTTCATCAAAATCAGG	*cdsA* upstream resequence
PgsA_updel_F	CTTTACTCCCTAAGCAAG	SM43 upstream of *pgsA* region amplification
PgsA_updel_R_PstI	ACGTCACTGCAGTCTACCAATAGTTAATACAT TAGG	SM43 upstream of *pgsA* region amplification
PgsA_dwndel_F_XmaI	ACGTCACCCGGGTTGTTGCTTGTTGAGACG	SM43 downstream of *pgsA* region amplification
PgsA_dwndel_R	GATCAAGAAGAACATGGA	SM43 downstream of *pgsA* region amplification
Erm_F_XmaI	ACGTCACCCGGGTAACGATCACTCATCATG	*erm* amplification from pG^{+}host4 plasmid
Erm_R_PstI	ACGTCACTGCAGCAAGTTAAGGGATGCAGT	*erm* amplification from pG^{+}host4 plasmid
PlsC_F_BacA	TGCATTTCAAAAATATTTTGAGGAGGAGTATC ATGTTTTATACTTATTTGC	SM43 *plsC* amplification for Gibson assembly, insert PbacA

PlsC_R	CATTTATAAGAAACTAGCTAAGGGATAATTGTA	SM43 *plsC* amplification for Gibson assembly
Cat_PlsC	AATTATCCCTTAGCTAGTTTCTTATAAATGG	Amplifies *cat* from pGR-*ermb* for Gibson assembly with *plsC*
PlsY_F_BacA	TGCATTTCAAAAATATTTTGAGGAGGAGTATC AGGTCTATGATGACATTTG	SM43 *plsY* amplification for Gibson assembly, insert PbacA
PlsY_R	CATTTATAAGAAACTCGTTTTATTTGTTAGG	SM43 *plsY* amplification for Gibson assembly
Cat_PlsY	CTAACAAATAAAACGAGTTTCTTATAAATGG	Amplifies cat from pGR-ermb for Gibson assembly with *plsY*
EV_Cat_F	TGCATTTCAAAAATATTTTGAGGAGGAGTATC AGTTTCTTATAAATGG	Amplifies pGR-*ermB* to remove *ermB* spacer to generate empty vector
BacA_R	GATACTCCTCCTCAAAATATTTTTGAAATGCAT TTCATTGCTATTATACCCA	Amplifies *rep* and PbacA from pGR-*ermB* for Gibson assembly
Rep_R	AATTCCTCATTTTCAGCAAATAACTCTTTTTC	Amplifies *rep* and PbacA from pGR-*ermB* for Gibson assembly
Cat_R	AAAAGAGTTATTTGCTGAAAATGAGGAATTAA A	Amplifies cat with cat_* primer for each acyltransferase from pGR-*ermB* for Gibson assembly
pGR_F	CTAAATAAAGAAAACCCACC	Acyltransferase insert amplification for sanger sequencing
pGR_R	CTAATTCTTGCGGAGTAACG	Acyltransferase insert amplification for sanger sequencing

Supplemental references

1. Akins RL, Katz BD, Monahan C, Alexander D (2015) Characterization of high-level daptomycin resistance in viridans group streptococci developed upon *in vitro* exposure to daptomycin. *Antimicrob Agents Chemother* 59(4):2102–2112.

2. Kilian M, Mikkelsen L, Henrichsen J (1989) Taxonomic Study of Viridans Streptococci: Description of *Streptococcus gordonii* sp. nov. and Emended Descriptions of *Streptococcus sanguis* (White and Niven 1946), *Streptococcus oralis* (Bridge and Sneath 1982), and *Streptococcus mitis* (Andrewes and Horder. *Int J Syst Bacteriol* 39(4):471–484.

3. Bridge PD, Sneath PH. (1982) *Streptococcus gallinarum* sp. nov. and *Streptococcus oralis* sp. nov. *Int J Syst Bacteriol* 32(4):410–415.

4. Lanie JA, et al. (2007) Genome sequence of Avery's virulent serotype 2 strain D39 of *Streptococcus pneumoniae* and comparison with that of unencapsulated laboratory strain R6. *J Bacteriol* 189(1):38–51.

5. Tettelin H, et al. (2008) Complete Genome Sequence of a Virulent Isolate of *Streptococcus pneumoniae*. *Science (80-)* 498(2001):498–507.

6. McBride SM, Fischetti VA, LeBlanc DJ, Moellering RC, Gilmore MS (2007) Genetic diversity among *Enterococcus faecalis*. *PLoS One* 2(7):e582.

7. Taylor RG, Walker DC, Mclnnes RR (1993) *E. coli* host strains significantly affect the quality of small scale plasmid DNA preparations used for sequencing. *Nucleic Acids Res* 21(7):1677–1678.

8. Biswas I, Gruss A, Ehrlich SD, Maguin E (1993) High-efficiency gene inactivation and replacement system for gram-positive bacteria. *J Bacteriol* 175(11):3628–3635.

9. Hullahalli K, Rodrigues M, Nguyen UT, Palmer K (2018) An Attenuated CRISPR-Cas System in *Enterococcus faecalis* Permits DNA Acquisition. *MBio* 9(3):e00414-18.